European Heart Journal – Cardiovascular Imaging (2016) **17**, 1071–1097
doi:10.1093/ehjci/jew172

EACVI/ASE EXPERT CONSENSUS DOCUMENT

Three-dimensional echocardiography in congenital heart disease: an expert consensus document from the European Association of Cardiovascular Imaging and the American Society of Echocardiography

John Simpson*, Leo Lopez, Philippe Acar, Mark Friedberg, Nee Khoo, Helen Ko, Jan Marek, Gerald Marx, Jackie McGhie, Folkert Meijboom, David Roberson, Annemien Van den Bosch, Owen Miller, and Girish Shirali

Evelina London Children's Hospital, London, UK

Received 31 May 2016; accepted after revision 28 June 2016

Three-dimensional echocardiography (3DE) has become important in the management of patients with congenital heart disease (CHD), particularly with pre-surgical planning, guidance of catheter intervention, and functional assessment of the heart. 3DE is increasingly used in children because of good acoustic windows and the non-invasive nature of the technique. The aim of this paper is to provide a review of the optimal application of 3DE in CHD including technical considerations, image orientation, application to different lesions, procedural guidance, and functional assessment.

Keywords EACVI • ASE • recommendation • three-dimensional echocardiography • congenital heart disease

Introduction

Three-dimensional echocardiography (3DE) has become important in the management of patients with congenital heart disease (CHD), particularly with pre-surgical planning, guidance of catheter intervention, and functional assessment of the heart. 3DE is increasingly used in children because of good acoustic windows and the non-invasive nature of the technique. The aim of this paper is to provide a review of the optimal application of 3DE in CHD including technical considerations, image orientation, application to different lesions, procedural guidance, and functional assessment.

Three-dimensional echocardiographic imaging techniques

Transducers

The evolution of 3DE techniques and transducer technology has been well described.[1–3] The development of the matrix array probe with parallel processing has made real-time 3DE possible since the 1990s.[4,5] Later generations of transducers have become smaller with footprints similar to two-dimensional echocardiography (2DE) transducers. The development of a small high-frequency paediatric 3DE transducer (2–7 MHz) has enhanced spatial and temporal resolution, especially pertinent for small children with high heart rates.[6,7] Similarly, miniaturization has enabled the development of adult-size 3D transoesophageal echocardiography (TOE) probes.[8]

Workflow

Ideally, 3DE transducers should be capable of producing 2D images which are at least equivalent to 2DE transducers. Some 3D transoesophageal transducers achieve this, but transthoracic 3DE probes still do not generally match the image quality of a dedicated 2D transducer. The difference remains most marked for high-frequency paediatric 3DE probes compared with the 2DE equivalent transducer. Consequently, the use of the combined 2DE–3DE transducer is not routine in smaller patients. Manufacturer recommendations suggest that current 3D TOE probes are used for

* Corresponding author. Tel: +44 2071882308; Fax: +44 2071882307. E-mail: john.simpson@gstt.nhs.uk

patients >30 kg. Some paediatric cardiologists will extend use of such probes to smaller patients. Those undertaking such procedures should be aware of the specific manufacturer recommendation for the transducer. In any patient, the risk of complications such as damage to the oropharynx and oesophagus caused by an oversized probe needs to be balanced against the additional value of 3DE. For patients who are currently too small to accommodate 3D TOE transducers, epicardial 3D imaging with a transthoracic 3DE transducer is a feasible alternative technique during surgery.[9]

Data acquisition modes

Good spatial and temporal resolution in 3DE is a priority for imaging of CHD, particularly valve pathology and complex lesions. The matrix transducer has different modalities of data acquisition whose use is dictated by the clinical question. For example, in the assessment of double outlet RV, the incorporation of the AV valves, ventricular septum, and great arteries is necessary for decision-making, whereas measuring the size of an isolated VSD does not require such an extended field of view. The exact configuration and nomenclature of different modes is vendor specific but with features in common.

2D simultaneous multiplane mode

Current matrix probes allow 360° electronic rotation of the imaging plane as well as simultaneous display of more than one 2D imaging plane that can be electronically steered in the elevation or lateral plane. The crop plane is marked on the projection but with the drawback that temporal resolution is reduced.[10] Applications include assessment of atrial septal defect (ASD) size and rim length,[11] size and shape of VSDs, AV valve morphology and regurgitation (*Figure 1A* and *B*), outflow tracts and arterial valves.

Real-time 3DE mode

Real-time 3DE permits a display of an adjustable pyramidal volume, minimizing the issue with poor co-operation in children because there is no potential for 'stitch' artefacts between adjacent subvolumes. Increasing the region of interest decreases frame rate, and the limited field of view is a disadvantage for complex CHD where the relationship of different structures to each other is crucial for decision-making. Some manufacturers have a further 3D mode which permits the operator to select an area of interest but with relatively low frame rates particularly if colour flow Doppler is added. This mode is mainly used during catheter intervention, particularly ASDs, VSDs, and the AV valves. Depending on the system, vendor settings may be adjusted to allow the operator to prioritize volume rate at the expense of line density, thus achieving a higher temporal but lower spatial resolution.

ECG-gated multi-beat acquisition

With current imaging technology, ECG-gated multi-beat image acquisition is frequently used for paediatric 3DE because it acquires a large field of view with sufficient temporal resolution. However, the electronic 'stitching' of narrow volumes of data over 2–6 heartbeats may produce artefacts related to patient breathing or movement, particularly in young children. This is not an issue in ventilated children under general anaesthesia, because ventilation can be suspended briefly, and is less of a problem during sleep or with sedation. Although 'single-beat' volume acquisition has been introduced, the limited temporal resolution is insufficient for high heart rates of infants and children unless the region of interest is small thereby permitting narrowing of the imaging sector, or if the region of interest is relatively static.

3DE colour flow Doppler

3DE colour flow Doppler can be added to any of the above modalities. In common with 2DE, the addition of colour flow Doppler reduces temporal resolution. Depending on the size of the region of interest, the achievable frame rate may be too low for fast moving structures such as AV valves. Some manufacturers may permit the user to prioritize temporal resolution over spatial resolution to maintain an acceptable frame rate. The alternative is to use an ECG-gated multi-beat acquisition to maintain an acceptable frame rate.

Principles of 3DE acquisition

3DE for CHD utilizes the same transducers and ultrasound systems as adults with the addition of high-frequency probes suitable for imaging babies and children. General points are summarized below with emphasis on points relevant to the child or adult with CHD. In all patients, meticulous attention to 2D image quality is necessary to optimize the quality of the 3DE dataset. A high-frequency 3DE transducer should be used where possible, especially in small children where ultrasound penetration is not an issue, and the sector width narrowed to include only the regions of interest. Axial resolution is higher than either lateral or elevational planes which impacts on the optimal transducer position for the lesion being evaluated. For example, the mitral valve may be interrogated either from apical or parasternal view to delineate both leaflets and the subvalvar apparatus.[12] Review of the multiplanar images is particularly important prior to display of rendered images to avoid diagnostic error. Comprehensive reviews of 3DE artefacts have been published for reference.[13]

Imaging of relatively static cardiac structures, such as ASDs and VSDs, may be achieved using live 3DE or 3DE 'zoom' modes because temporal resolution is sufficient. Gain settings during acquisition and post-processing are particularly important in smaller patients with thin valves to reduce 'noise' that may impede visualization (*Figure 2A* and *B*) while avoiding 'holes' or other artefacts from inadequate gain. The normal gain setting for a 3DE acquisition is slightly higher than conventional 2DE as gain can be reduced during post-processing to optimize the image, whereas if too little gain is used during acquisition, increasing gain during post-processing does not restore parts of the image which have not been adequately visualized during the acquisition. This affects thin structures such as valve leaflets in particular.

Presentation of 3DE images of CHD merits particular consideration, especially for valves, and individualized tilt or rotation to display the region of interest can help (*Figure 3A* and *B*). The 3D display modes for CHD are analogous to those used for adults and include (i) volume rendering, (ii) surface rendering, and (iii) multiplanar reformatted (MPR) image display.[14,15] Volume-rendered datasets can be electronically segmented, allowing the operator to 'crop' the heart in multiple sections to expose the cardiac structure of interest from any desired angle. This is especially useful for CHD prior to surgery or intervention. Surface rendering presents the surfaces of

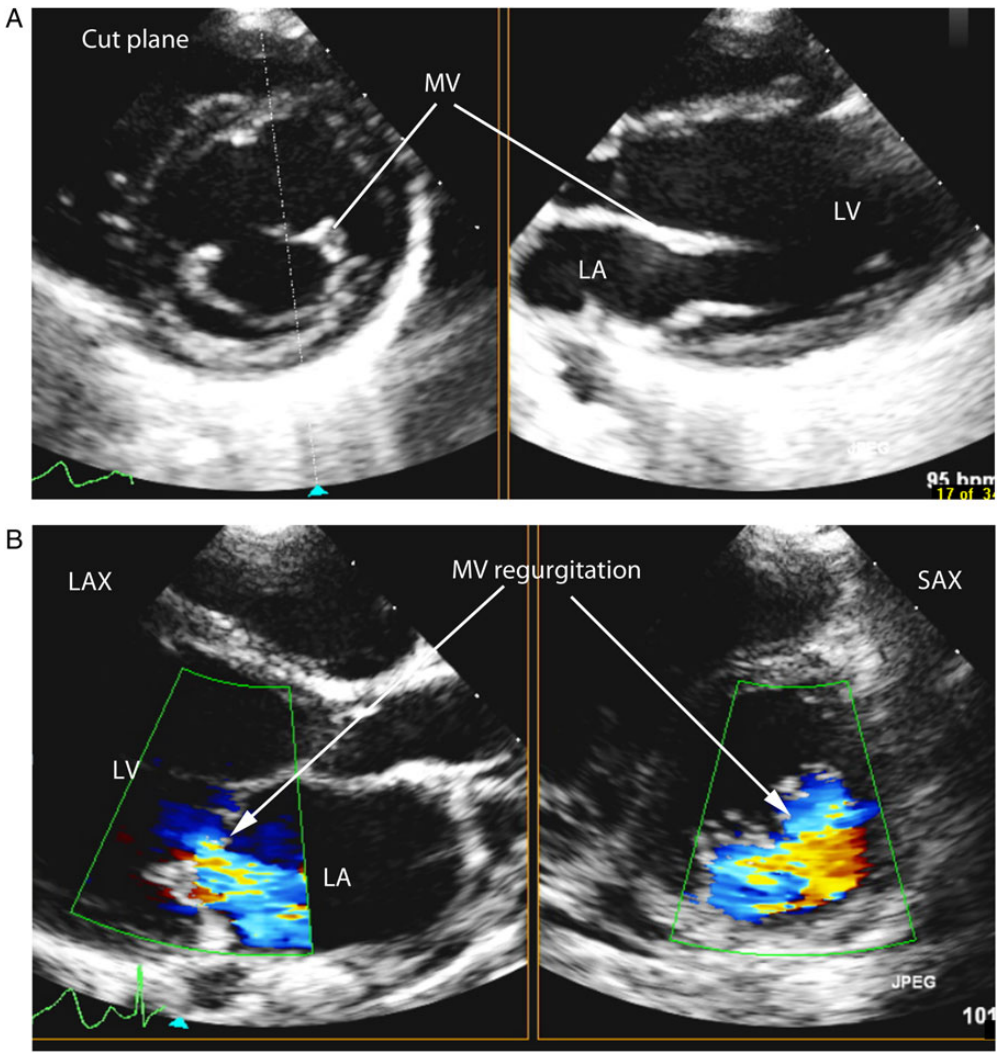

Figure 1 Cross-plane imaging. (*A*) Cross-plane imaging of the mitral valve by transthoracic echocardiography showing the user defined cut plane (dotted line and triangle) to show a short-axis view of the mitral valve (left panel) and the corresponding long-axis view (right panel). (*B*) Cross-plane imaging of mitral valve regurgitation which permits precise localization of regurgitant jets in the long-axis (left panel) and short-axis views (right panel). The cut plane is indicated by the blue triangle. LAX, long axis; SAX, short axis; LV, left ventricle; LA, left atrium; MV, mitral valve.

structures or organs with a solid appearance and is mainly used to visualize size, shape, and function of cardiac structures.[16] Analysis software for this mode includes semi and fully automated endocardial border detection for quantification of left ventricular (LV) and RV function[17,18] as well as semi-automated mitral leaflet motion detection for quantification of valve function, both of which may be limited by the abnormal ventricular shape or valve morphology found in CHD.

MPR allows the 3DE dataset to be viewed on a quad screen with the 3D dataset cut into three planes (sagittal, coronal, and transverse) which are configurable by the user. Adjustment of the MPR planes is illustrated in see Supplementary data online, *Powerpoint 1*. This display of planes not available by 2DE can aid with understanding complex anatomies and facilitate measurement of many CHDs such as ASD and VSD size. Valve areas, effective orifice areas, and *vena contracta* areas of regurgitant jets can all be measured by manipulating cutting planes to avoid foreshortening or oblique measurements.[19–21]

Future directions

Improved temporal resolution of single-beat acquisitions or post-processing software to deal with stitch artefacts would enhance 3DE in younger patients. Software packages that can accommodate analysis of valves and chambers of abnormal morphology would also benefit the patient with CHD.

Recommendations

The 3DE approach should be tailored according to the patient. Small footprint and high-frequency 3DE transducers should be used in infants and young children and for epicardial 3DE.

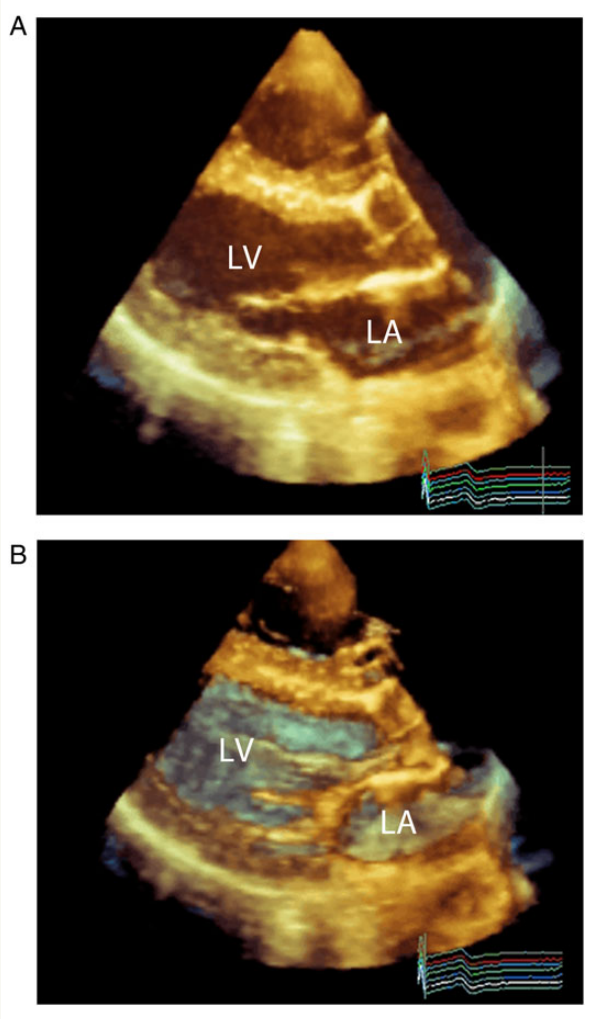

Figure 2 Effect of gain setting on 3D images. (*A*) Transthoracic PLAX view of the LV with inappropriately high gain settings. The cavity of the left atrium and left ventricle is opaque and consequently there is no perception of depth in the image. (*B*) With appropriate reduction of gain, intracavity noise has been removed and far-field structures can be visualized. In this example, far-field structures are colour coded blue grey and near field brighter and yellow-brown. LV, left ventricle; LA, left atrium.

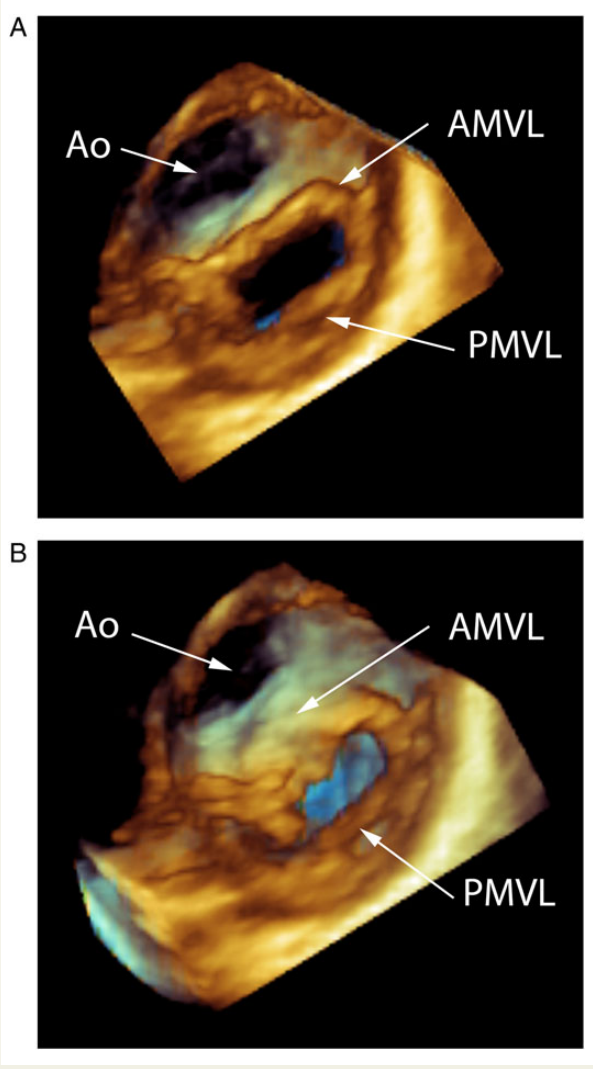

Figure 3 Rendered views of the mitral valve by transthoracic 3DE. (*A*) This is a projection of a normal mitral valve viewed from the ventricular aspect. The mitral valve is viewed directly en face so that the leading edge of the anterior and posterior leaflets can be visualized along with the aorta in the far-field. (*B*) This is a similar projection of the mitral valve to that shown in (*A*). However, the rendered image has been angulated slightly so that the depth of the anterior leaflet of the mitral valve can be visualized. This assists in imaging of abnormalities in this region such as true clefts of the mitral valve or the bridging leaflets in atrioventricular septal defects. Ao, aorta; AMVL, anterior mitral valve leaflet; PMVL, posterior mitral valve leaflet.

3D TOE should be considered when patient size permits if 3D TTE provides insufficient imaging to plan therapy.

Image display and orientation

Published standards have been produced for the echocardiographic assessment of patients with paediatric and CHD, including TTE,[22] TOE,[23] and quantification.[24] Recent published work has defined standards for adult practice using 3DE,[14] but the latter specifically excluded CHD. In the patient with CHD, cardiac position, situs, connections, and alignments may be abnormal which presents a major challenge compared with acquired heart disease. 3DE facilitates *en face* projections of cardiac septums and AV valves,[25] which can be rotated in the *z*-plane to any desired orientation. If the analogy of a clock face is used, the use of *z*-plane rotation turns the image in a clockwise or counter clockwise direction to achieve an anatomically correct orientation (see Supplementary data online, *Presentation 1*). The retention of adjacent anatomic landmarks is desirable, where possible, to assist orientation. Echocardiographic evaluation of the patient with CHD is often complemented by other imaging modalities including magnetic resonance imaging (MRI), computed

tomography (CT), and angiography. To gain maximum value, the orientation of 3DE images should be both consistent and intuitive, as exemplified by the 'anatomic' approach to image display,[26] projecting the heart in the same orientation as a person standing in an upright position. With this approach, superiorly positioned structures will be displayed uppermost on the image. This anatomically correct approach is consistent with the projection of MRI and CT images.[26,27] The application of an anatomic orientation can be illustrated with specific examples.

The atrial septum

The atrial septum can be visualized from the right or left atrial aspect. A projection from the right atrium permits visualization of important landmarks such as the superior vena cava, inferior vena cava, ascending aorta, tricuspid valve, oval fossa, and os of the coronary sinus. The preferred anatomic image orientation has the superior vena cava uppermost and tricuspid valve seen to the right of the atrial septum (*Figure 4*).

The ventricular septum

The ventricular septum can be visualized from either the RV or the LV aspect. By convention, the components of the ventricular septum are named as if the septum is viewed from the RV side with the free wall of the RV removed. With the anatomic approach, the diaphragmatic border of the heart is lowermost, the RV apex is seen to the right and the RV outflow tract viewed uppermost on the projected image so that landmarks such as the tricuspid valve, moderator band, and septomarginal trabeculation are seen in anatomically appropriate position (*Figure 5A*). Similarly, the LV aspect of the ventricular septum can be viewed in an anatomic projection (*Figure 5B*), to include both the septum and LV outflow tract.

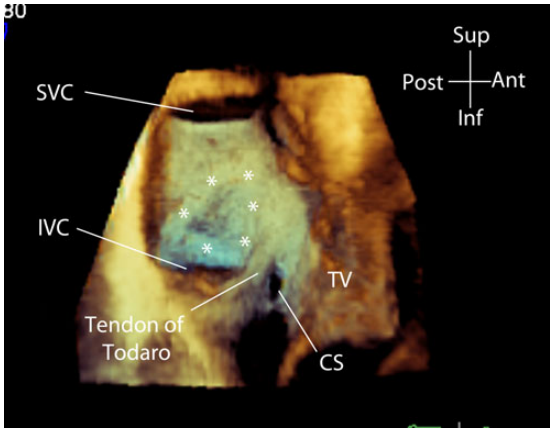

Figure 4 Normal atrial septum. Transoesophageal 3DE view of the normal atrial septum viewed from the right atrial aspect. The orientation of the image is anatomic so the superior vena cava and inferior vena cava are shown uppermost and lowermost on the image respectively. This image was acquired by 3D TOE using a full-volume acquisition over four cardiac cycles. The asterisk marks the margins of the oval fossa. SVC, superior vena cava; IVC, inferior vena cava; TV, tricuspid valve; CS, coronary sinus.

AV valves

In CHD, the left-sided AV valve may not be a bileaflet valve of 'mitral' type and the right-sided AV valve may not be the tricuspid valve. Regardless of the morphology of the valve, or whether an *en face* view is projected from the ventricular or atrial aspect, the 3D rendered image is rotated so that the diaphragmatic surface of the heart is shown lowermost (*Figure 6A* and *B*). This means, for example, that

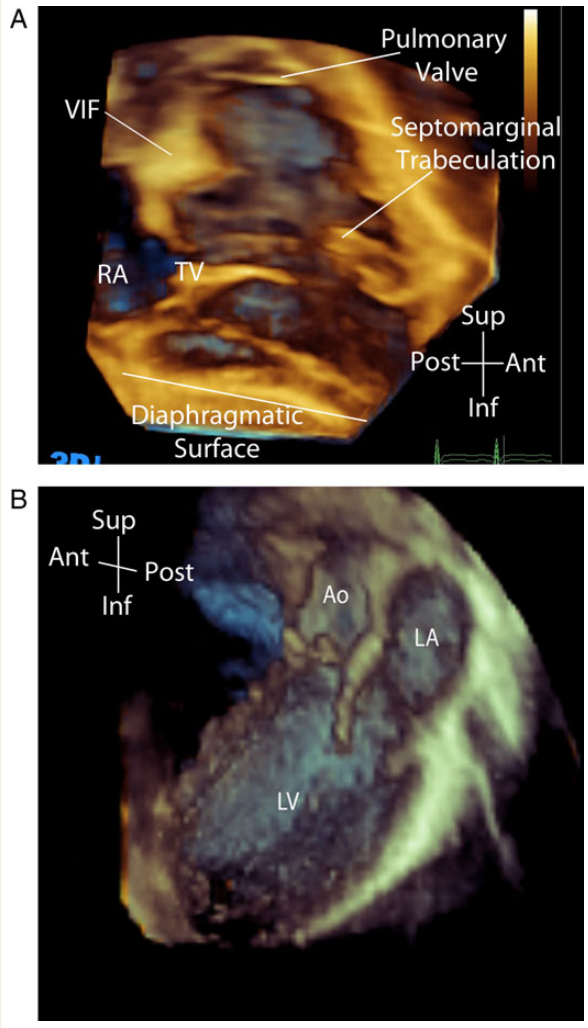

Figure 5 (*A*) Transthoracic rendered 3DE image of the right ventricular side of the normal ventricular septum. The free wall of the right ventricle has been cropped away in post-processing. The important landmarks can be readily identified including the tricuspid valve (TV), ventriculo-infundibular fold (VIF), and septomarginal trabeculation (septal band). This type of view can be used to project all types of ventricular septal defects. (*B*) Left side of the normal ventricular septum. A full-volume 3DE dataset was obtained by transthoracic 3DE in a paraseternal long-axis view. The free wall of the left ventricle has been cropped away so that the ventricular septum can be directly visualized from the LV cavity. The smooth wall of the left ventricle can be appreciated. VIF, ventriculo-infundibular fold; RA, right atrium; TV, tricuspid valve; Ao, aorta; LA, left atrium; LV, left ventricle.

the superior bridging leaflet in an AV septal defect will be shown uppermost on the image and the inferior bridging leaflet lowermost (*Figure 7*).

Aortic and pulmonary valves

The morphology, position and patency of the aortic, and pulmonary valves cannot be assumed in CHD. These valves are therefore projected in an anatomic format using the standard conventions for nomenclature of the valve leaflets. For example, the aortic valve may be projected as if seen from the ascending aorta or from the LV outflow tract. The conventional nomenclature of left, right, and non-coronary leaflets and sinuses is used in exactly the same fashion as in 2DE. An example of the preferred orientation of the aortic valve is shown (*Figure 8*) and a similar approach is used for the pulmonary valve.

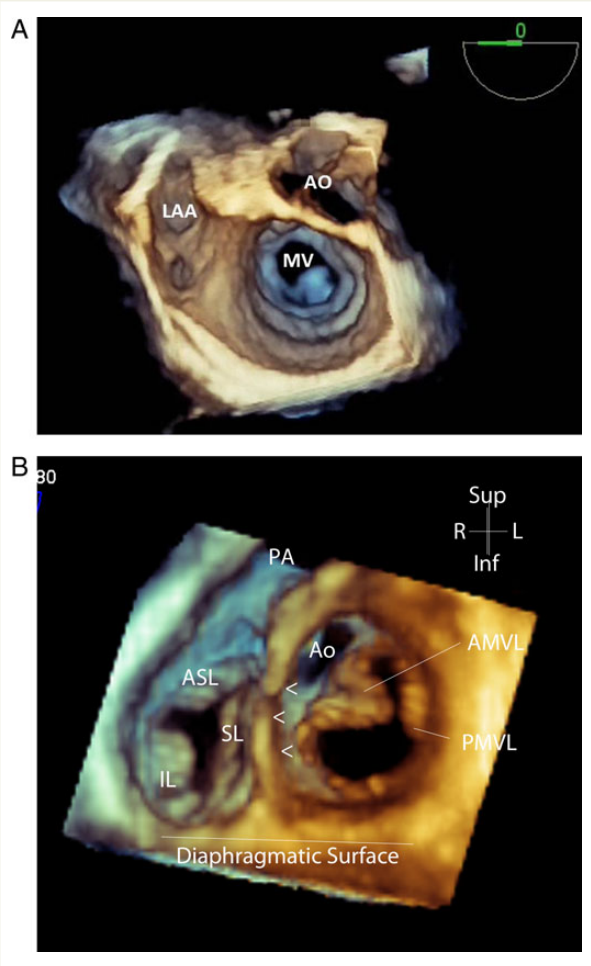

Figure 6 (*A*) Transoesophageal 3DE view of the mitral valve from the atrial side. The mitral valve, aortic valve, and left atrial appendage are visualized from the atrial aspect in an anatomic orientation. If the annulus of the mitral valve is viewed as a clockface, the aortic valve is at 2 o'clock with reference to the mitral valve. (*B*) Transosophageal 3DE view of the mitral and tricuspid valves from the ventricular side. The mitral and tricuspid valves are viewed from the ventricular aspect in an anatomic orientation. The aorta is at a 10 o'clock position with reference to the mitral valve. The inferior, septal, and anterosuperior leaflets of the tricuspid valve are seen in anatomic orientation as well as the curved shape of the ventricular septum. LAA, left atrial appendage; MV, mitral valve; ASL, anterosuperior leaflet of the tricuspid valve; IL, inferior leaflet of the tricuspid valve; SL, septal leaflet of the tricuspid valve; PA, pulmonary artery; Ao, aorta; AMVL, anterior mitral valve leaflet; PMVL, posterior mitral valve leaflet.

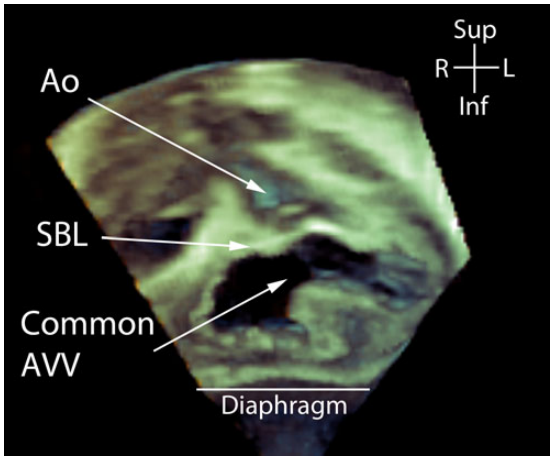

Figure 7 Transthoracic 3DE en face view of atrioventricular septal defect. En face view of a complete atrioventricular septal defect from the ventricular aspect, obtained using a subcostal view. The depth of field means that the superior bridging leaflet and the common atrioventricular valve are seen as well as the aorta in the far field. Ao, aorta; SBL, superior bridging leaflet; AVV, atrioventricular valve.

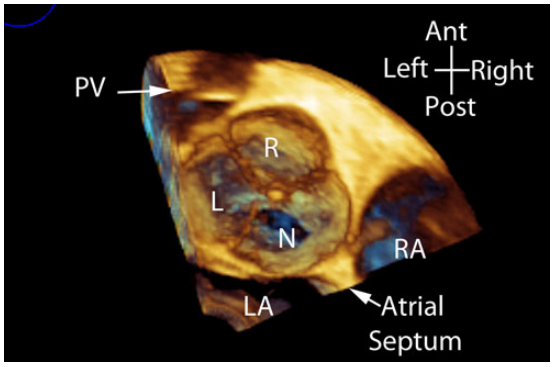

Figure 8 En face view of the normal aortic valve. Transoesophageal 3DE view of a normal aortic valve viewed from the aortic side of the valve. R, right coronary leaflet; L, left coronary leaflet; N, noncoronary leaflet; LA, left atrium; RA, right atrium; PV, pulmonary valve.

Complex abnormalities of cardiac connections

When the main cardiac connections are abnormal, an anatomic presentation of images is particularly important so that the abnormal anatomy is displayed in a manner as close as possible to the actual spatial locations. An accurate understanding of the relationship of intracardiac structures has a direct impact on the surgical approach.

'Surgical' views of the heart

The term 'surgical' view has been used to describe 3D projections that are most akin to the surgeon's view during an operation. There are specific considerations for this term, particularly in contrast to the 'anatomic' view. The anatomic view is projected as if the person is standing upright, whereas a surgical view is projected as if the patient is lying supine with the lead surgeon operating from the right side of the patient. The effect of this is that an anatomic *en face* view of the right side of the atrial or ventricular septum would be rotated counter clockwise 90° when projecting a 'surgical' view (*Figure 9*). Views of the atrial aspect of the AV valves are often referred to as 'surgical' even though the surgeon may take a different access route to repair the valve in question. For example, the truly surgical view of the mitral valve would be presented with the patient supine with the left atrium accessed through the atrial septum. This contrasts with the usual projected 3DE view obtained by cropping away the posterior aspect of the atriums and rotating the AV valves *en face* with rotation of the whole dataset into an anatomic position. In practice, our preference is an anatomic orientation, which maintains consistency with projections of MRI and CT scans, knowing that 'surgical' visualization of the structures may be different. A visual demonstration of the common manipulations of 3D datasets accompanies this document (see Supplementary data online, *Presentation 1*).

Future directions

The availability of orientation markers, already available for CT angiography and MRI, is needed for 3DE to mark, for example, the true left/right or superior/inferior orientation of an image. This should be coupled with the ability to 'landmark' important anatomical structures to enhance display of complex CHD as the data is manipulated. Fusion imaging, where 3DE datasets can be co-registered with datasets from other modalities (fluoroscopy, CT angiography, and MRI), will allow for both automated anatomic orientation of 3DE images and visualization of regions which may be sonographically inaccessible. Widespread implementation would require co-registration across vendors, modalities, and platforms.

Recommendations

An 'anatomic' approach to image display is recommended as it reflects the real position of structures in space and is consistent with other modalities such as MRI and CT.

En face views of septums and AV valves should retain important landmarks and be rotated into a correct anatomic orientation.

The term 'surgical' view should be used only for projections that show anatomy as the surgeon would visualize the region of interest.

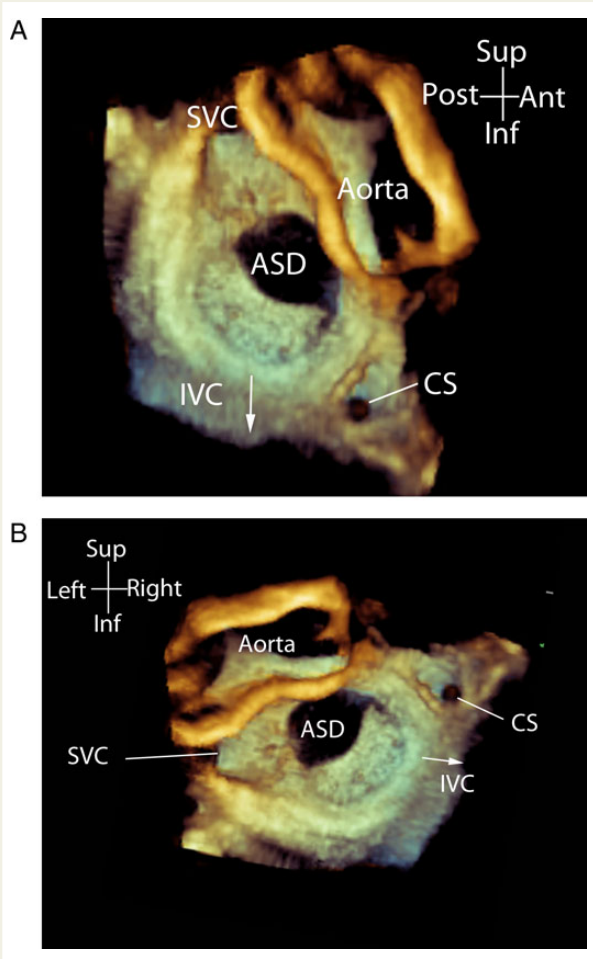

Figure 9 3D TOE views of 'Surgical' vs. anatomic views of an atrial septal defect. (*A*) Atrial septal defect viewed from the right atrial aspect in an anatomic orientation with the superior vena cava uppermost and inferior vena cava lowermost on the image. (*B*) Atrial septal defect viewed from the right atrial aspect in a 'surgical' orientation where the defect is viewed from the right side in an analogous fashion to the patient in a supine position. This amounts to a 90° anticlockwise rotation of the anatomic projection. SVC, superior vena cava; IVC, inferior vena cava; CS, coronary sinus.

Optimal sonographic projections for different congenital heart lesions

Standard imaging planes in 2DE have been developed from a combination of anatomical constraints and accessible sonographic windows, forming the basis for published standards.[22] 3DE is less constrained since post-processing will allow interrogation of structures contained within the acquired volume. A corollary is that a structure of interest can be displayed similarly after post-processing despite being acquired from a range of different echocardiographic windows. However, the principles of imaging physics apply as much to 3DE as they do to 2DE. For this reason, there are optimal

approaches for data acquisition that should allow for optimal demonstration of the structure of interest. General recommendations can be made about the optimal acoustic windows to show different regions of interest. These include the following:

(i) clear visualization of the region of interest on 2DE
(ii) insonation orthogonal to the plane of the structure of interest where possible
(iii) inclusion of clinically relevant adjacent structures
(iv) optimization of volume width and depth

For example, acquiring a 3D dataset to display an ASD is best achieved in a subcostal window because insonation from this view is orthogonal to the plane of the atrial septum. With TOE there is less flexibility to adjust the sonographic window; however, this is offset by higher image quality than TTE.[28]

Although image quality is central to interrogation of regions of interest and good 3D reconstruction, there are important differences from 2DE. For example, parasternal long-axis (PLAX) and parasternal short-axis (PSAX) views are used in 2DE to evaluate a perimembranous VSD (pmVSD) because the defect is in the near field, and good alignment to Doppler jets can be achieved. However, 3DE is especially useful for its ability to display VSDs *en face* and to delineate adjacent structures. PLAX and PSAX views are limited because of the small size of the ultrasound sector in the near field. Thus, subcostal and modified apical views may better define adjacent structures because the VSD is in the centre of the imaging field with a wider sector. This tailored approach is also employed for more complex lesions such as double outlet RV where AV valves, ventricular septum, and outlets all have to be incorporated into the 3DE volume.[29] *Table 1* summarizes optimal TTE sonographic views and the usefulness of 3D TOE for common forms of CHD.

Technical limitations may, however, persist irrespective of the imaging plane. Both the aortic and pulmonary valves are thin, rapidly moving structures. These are often imaged by 3D TTE using a PLAX or PSAX view where the plane of insonation does not lend itself to good quality rendering of the entirety of individual valve leaflets, particularly the body of the leaflet. This issue can be overcome by TOE in patients large enough to accommodate the 3D TOE probe.

Recommendations

Optimal sonographic projections for different congenital heart lesions

The angle of insonation should be tailored to the region of interest and ideally should be orthogonal to the relevant structure.

The size of 3DE region of interest should be adjusted to optimize temporal and spatial resolution.

Table 1 Suggested transthoracic acoustic windows and utility of 3DE for CHD

	Subcostal	Apical	PLAX	PSAX	3D-TOE
Atrial septum					
ASD	+++	+ (modified)	+ (modified)	+ (modified)	+++
SV ASD	+++	−			+++
AV junction					
AVSD	+++	+++	++ (LAVV)	+ (LAVV)	+++
Ebstein's/TV dysplasia	+++	++ (Anterior angulation)	+	++	+
MV chordal structure	−	+ (smaller patients)	+++	++	+++
Double orifice MV	++	++	+	++	++
MVP	−	++	+++	++	+++
Parachute MV	++	++	++	++	++
Supra mitral membrane	−	++	+++	+	+++
Ventricular septum					
mVSD (except anterior defects)	+++	++	+	+	++
Membranous VSD	+++	+	+	+	++
Doubly committed subarterial VSD	++	−	++ (Angled to PA)	+	++
Outlets					
Aortic valve	−	+	++	++	+++
Pulmonary valve	−	+	−	+	++
Double outlet right ventricle	+++	+	−	+	+

PLAX, parasternal long axis; PSAX, parasternal short axis; ASD, atrial septal defect; SV, sinus venosus; AVSD, atrioventricular septal defect; LAVV, left atrioventricular valve; TV, tricuspid valve; MV, mitral valve; MVP, mitral valve prolapse; VSD, ventricular septal defect; PA, pulmonary artery.

Added value of 3DE for different congenital heart lesions

The literature on application of 3DE to CHD covers a wide variety of lesions including the AV valves, atrial septum, ventricular septum, and the outflow tracts. The use of 3DE techniques has increased as technology has improved, but there is wide institutional variability in the adoption of the technique. A central point in this regard is the evidence of additional diagnostic information compared with either 2DE or other imaging modalities. There have been no randomized trials relating to procedural success, morbidity or mortality related to the application of 3DE. Rather, 3DE has been adopted into practice on the basis of a clinical need to provide additional diagnostic information. *Tables 2* and *3* present our consensus view of the added value of 3DE to assess some major groups of lesions. A selection of the key references relating to each of the different lesions is also included within the tables as well as a summary of the additional information provided. The type of lesions for which 3DE has a major role is heavily weighted towards valvar lesions and defects in both the atrial and ventricular septum (see Supplementary data online, *Appendix 1, Presentation 1*). A good example of the application of 3DE to more complex CHD is decision-making in patients with double outlet RV where particular considerations include the size and location of the VSD, and the relative position of the great arteries (*Figure 10A–D*, Supplementary data online, *Video 1A–D*). The depth of field enhances visualization of the position and size of the VSD relative to the great arteries, and projections are achieved from the RV aspect and apex which cannot be achieved by 2DE.

Recommendations

Added value of 3DE for different congenital heart lesions

3DE is recommended for the assessment of valvar lesions, septal defects, and complex abnormalities of the cardiac connections.

3DE should be regarded as a technique that complements rather than replaces 2DE for assessment of CHD.

Table 2 Use of 3DE in congenital lesions with normal cardiac connections

Region of interest	3D modalities	Information acquired (I) Comment (C)	Strength of recommendation
Atrial septum	GS/CFM TTE/TOE	I: Size/number/shape /location of defects C:High value for multiple defects, multiple device deployment, residual leaks, spiral defects	HIGH for complex or residual defects MODERATE for single central defects LOW for PFO[11,11,28,30–33]
Tricuspid valve abnormality	GS/CFM TTE/TOE	I: Leaflet morphology Chordal support Delineation of regurgitant jets C: Mechanism/severity of regurgitation refined	HIGH[34–39]
Mitral valve	GS/CFM TTE/TOE	Leaflet morphology Chordal support Delineation of regurgitant jets C: Mechanism/severity of regurgitation refined	HIGH[9,12,40–42]
Ventricular septum	GS/CFM TTE/TOE	I: Size/number/shape /location of defects C:High value for multiple defects, unusually located defects or consideration of interventional closure	HIGH for more complex defects LOW for other defects[43–48]
Left ventricular outflow tract	GS/CFM TTE/TOE	I: Morphology of subaortic obstruction and aortic valve C: Clarify mechanism of obstruction and/or regurgitation	HIGH[19,49,50]
Aortic valve	GS/CFM TTE/TOE	I: Measurement of aortic valve Morphology of aortic valve leaflets Mechanism of aortic regurgitation C: Imaging of aortic valve leaflets more difficult by 3D TTE, 3D TOE preferred	HIGH Especially by TOE[21,51,52]
Aortic arch	GS/CFM TTE	I: Morphology and sizing of aortic arch C: Imaging may be difficult due to probe size, acoustic access	LOW/MOD[53]
Right Ventricular Outflow tract	GS/CFM TTE/TOE	I: RVOT morphology Visualization of site of RVOT obstruction C: Questionable benefit over 2DE	LOW /MODERATE[54,55]
Pulmonary valve	–	I: PV morphology and function C: May be able to visualize PV morphology better than 2DE	Low[54,55]
Branch pulmonary arteries	–	Not routinely used	None

GS, greyscale; CFM, colour flow mapping; TTE, transthoracic echocardiography; TOE, transoesophageal echocardiography.

Table 3 Use of 3D echo for the heart with abnormal cardiac connections

Abnormal cardiac connection	3D modalities	Information acquired (I) Comment (C)	Strength of recommendation
Systemic venous abnormalities	–	Not routinely used	No recommendation
Abnormal pulmonary venous drainage	–	Not routinely used	No recommendation
Atrioventricular septal defect	GS/CFM TTE/TOE	I: Size of atrial and ventricular components of the defect Leaflet morphology and chordal support Delineation of regurgitant jets Valvar and ventricular size in unbalanced defects C: Enhances measurement of valve size, chordal support and relative size of AV valves and ventricles	HIGH[9,40,41,56–59]
Discordant atrioventricular connections	GS/CFM TTE/TOE	I: TV and MV morphology and function Location and size of associated VSDs Right and LV outflow tract C: Improves assessment of feasibility of Senning/Rastelli approach. Improves localization of VSDs	HIGH[60,61]
Simple transposition of the great arteries	–	Not routinely used	No recommendation
Complex transposition of the great arteries	GS/CFM TTE/TOE	I: MV and TV morphology and size. Size, location of associated VSDs Anatomy of left or RV outflow tract obstruction C: Suitability for procedures such as Rastelli, Nikaidoh and arterial switch operations	HIGH[62,63]
TOF	GS/CFM TTE	I: VSD size/location and RVOT anatomy C: Indicated where specific concerns, e.g. VSD position or RVOT anatomy More extensive use for RV volume estimation postoperatively	LOW
Common arterial trunk	GS/CFM TTE/TOE	I: Truncal valve morphology/regurgitation C: Not routinely indicated in infancy May assist delineation of truncal valve morphology/regurgitation in older patients by TEE	HIGH for truncal valve in older patients LOW in infancy
Double outlet RV	GS/CFM TTE	I: Relationship of AV valves VSD size and location Relative position of great arteries C: High value for guiding appropriate type of repair	HIGH[29,63]

GS, greyscale; CFM, colour flow mapping; TTE, transthoracic echocardiography; TOE, transoesophageal echocardiography.

Use of 3DE to guide catheter intervention

3D TOE is a rapid and useful imaging technique for the assessment of CHD during catheter-based interventions, including device closure of ASDs[11,28,30–33,64–68] and VSDs.[43–45,68,69,70] 3D TOE complements rather than replaces 2D TOE, and both modalities are used to assess defects and adjacent margins, rims, and structures. 3DE is particularly helpful for irregularly or asymmetrically shaped defects where 2D assessment of size by rotation of the TOE probe is insufficient. *En face* views of defects permit more precise appreciation of adjacent structures than 2D TOE alone, particularly for more complex lesions. 3D TOE of younger patients is typically done under general anaesthesia and is only feasible in patients large enough to accommodate the 3D TOE probe. Current manufacturers' recommendations propose a minimum patient weight of 30 kg. Time is limited during the procedure; therefore, rapid, simple, and minimal post-processing real-time 3D acquisition modes are often most effective. A 3D full-volume acquisition is favoured at some centres to produce a high-resolution view of the entire region of interest at the start of the procedure, followed by more focused imaging using live techniques. Lesion-specific targeted views have to be obtained, as discussed in subsequent sections. *En face* views are consistently used to demonstrate the relevant anatomy and interventional hardware. In addition to rendered 3D views, MPR imaging is useful for quantitation and image display during interventions[19] (*Figure 10*).

ASD device closure

Transcatheter device closure of a secundum ASD has become the preferred method of treatment when the anatomy is favourable.[71,72] Accurate assessment of ASD type, size, position, number of orifices, shape, and rim sizes (*Figure 11*) is essential for correct patient selection, device selection, and deployment. Detailed analysis of device position, configuration, anchorage, residual shunt as well as the relationship of the device to the aorta, mitral valve, tricuspid valve,

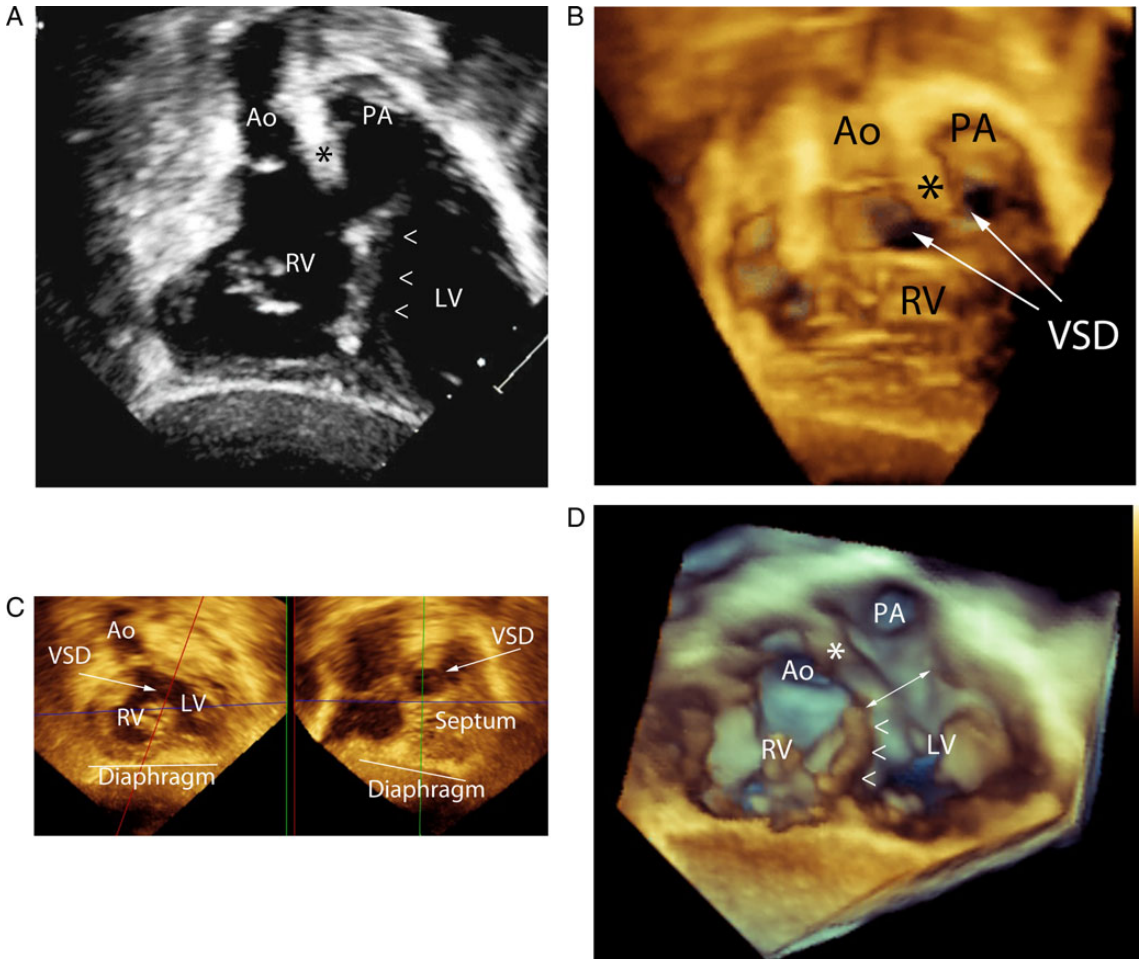

Figure 10 Transthoracic 3DE of double outlet right ventricle from a subcostal projection using a multi-beat acquisition. (*A*) Subcostal 2D echocardiographic view of double outlet right ventricle. The plane of the ventricular septum is shown by the arrows (<) and the outlet septum between the aorta and the pulmonary artery is shown by the asterisk. Note that the ventricular septal defect is not visualized as the outlet septum is entirely within the right ventricle and the plane of the ventricular septum would be posterior to the plane used in this image. (*B*) Subcostal 3D echocardiographic image of the same patient. The aorta (Ao) and the pulmonary artery (PA) are separated by the outlet septum (*). Due to the depth of field provided by the 3D image, the margins of the ventricular septal defect are clearly visualized. This is clinically important because the size and position of the ventricular septal defect may determine whether the left ventricle may be baffled to the aorta as part of the surgical repair. (*C*) MPR images showing the relationship of the ventricular septal defect to the aorta. The red plane is en face to the ventricular septal defect which is profiled in the right panel. This permits accurate measurement of the size of the ventricular septal. (*D*) 3D rendered image from the ventricular apex. The left ventricle and right ventricle are shown in short axis. The ventricular septum is shown by the arrowhead (<) and the ventricular septal defect is shown by the double-headed arrow. The depth of field of this projection shows the location of the ventricular septal defect, the outlet septum (*), and the relative position of the great arteries. Ao, aorta; PA, pulmonary artery; LV, left ventricle; RV, right ventricle.

superior and inferior vena cava, and the pulmonary veins is necessary (*Figure 11*). Demonstration of these features is usually enhanced and at times only possible with 3DE.[30,31,64–67,73]

The 3D TOE right atrial *en face* views from the mid-oesophagus selecting the region of interest to produce real-time 3D images can often demonstrate the key features during secundum ASD intervention. 3D full-volume acquisition may be needed if the volume rate using focused live 3D acquisition is too low. The deep trans-gastric sagittal bicaval view best demonstrates the inferior rim and septal length and provides a good view from which to monitor device deployment. Precise measurement of the ASD is best performed using the MPR four panel format, but measurement of the rendered image is an alternative (*Figure 10*). Colour Doppler flow analysis of the size, position, and mechanism of residual shunts is best performed with live 3D colour or biplane imaging. There are reports of using transthoracic 3DE to guide ASD closure from a subcostal view.[73,74]

VSD device closure

Transcatheter closure of VSDs has developed as an alternative treatment to surgical closure of muscular VSDs (mVSDs) and pmVSDs.[75–81] Specific advantages of 3DE over 2DE are improved visualization of the VSD shape, size, and location as well as

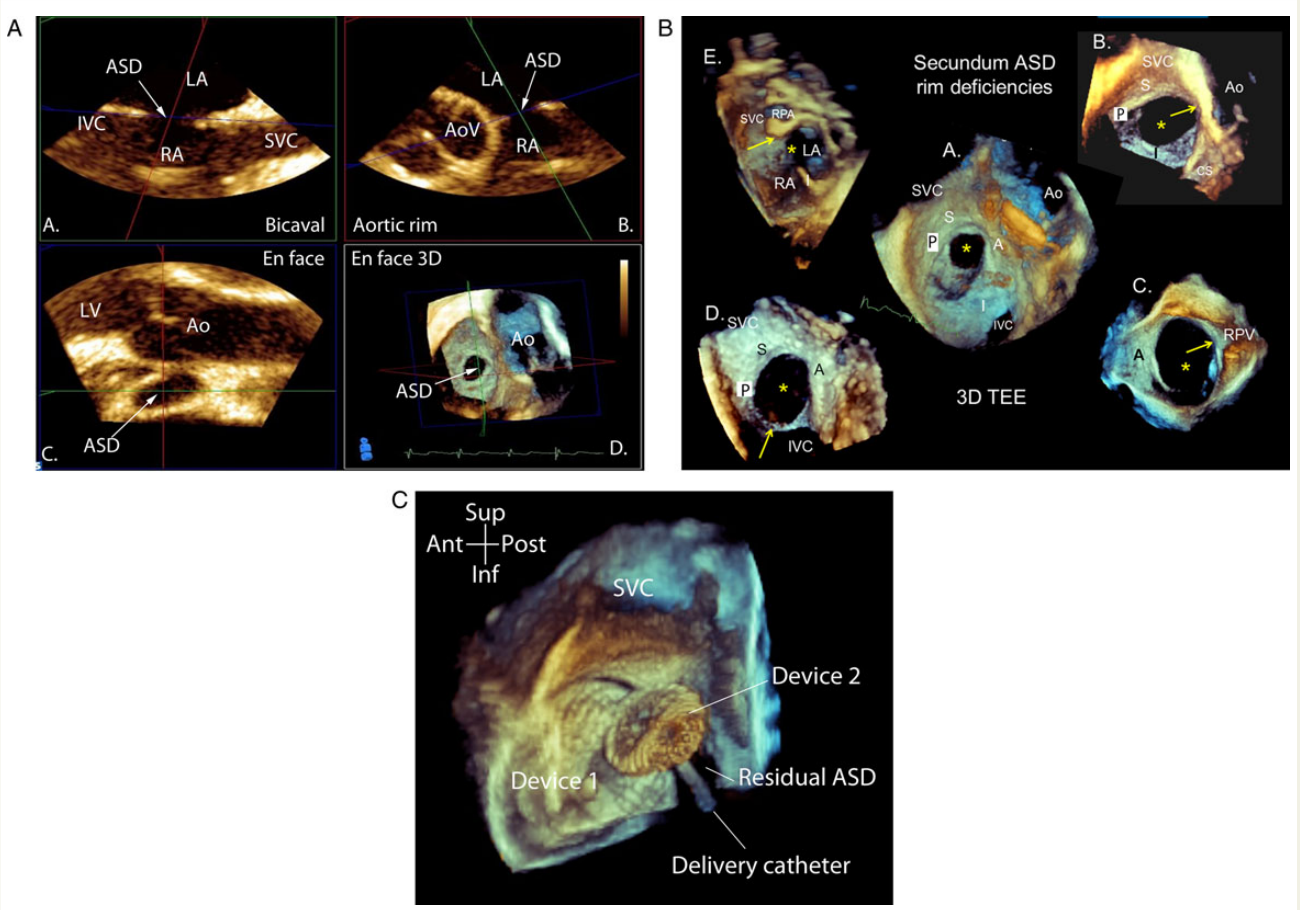

Figure 11 (*A*) 3D transoesophageal projection of MPR images of a secundum atrial septal defect. The blue plane is orientated to include the margins of the defect (*A* and *B*) which defines the en face projection shown in cross-section in (*C*) and rendered view in (*D*). The rims of the defect can be measured either on the MPR images or rendered image. (*B*) Transoesophageal 3DE rendered images of the morphology, size and rims of the atrial septal defect (*) of atrial septal defects with deficient rims in different regions. The zones where there is a deficient rim are marked with an arrow. The rims appear adequate throughout (*A*), deficient aortic rim (*B*), deficient right pulmonary vein rim (*C*), deficient inferior vena caval rim (*D*), and superior vena caval rim (*E*). Images (*A*), (*B*), and (*D*) are viewed from the right atrial side and Image (*C*) from the left atrial side. Image (*E*) cuts through the atrial septum so that the crest of the septum and the superior position of the defect can be visualized. (*C*) Transoesophageal real-time 3DE image of deployment of a second septal occluder to close a residual atrial septal defect. This 3D rendered projection from the left atrial aspect shows the relative position of the two septal occluders, the residual defect and the delivery catheter. SVC, superior vena cava; IVC, inferior vena cava; LA, left atrium; RA, right atrium; Ao, aorta; RPV, right upper pulmonary vein; S, superior; P, posterior; A, anterior; I, inferior; LV, left ventricle; ASD, atrial septal defect; AoV, aortic valve; MPR, multiplanar reformatted.

characterization of the tricuspid pouch and surrounding structures.[43,44,46,68–70] *En face* presentation of the ventricular septum from both RV and LV aspects can be accomplished most expeditiously from a four-chamber view using live 3D (*Figure 12*) or ECG-gated full-volume acquisition. Monitoring of interventional device hardware and device deployment is seen in a frontal four-chamber view (*Figure 12*). Following device deployment, live 3DE, cross plane, or MPR imaging with colour flow Doppler is optimal for assessing the interventional result.

Additional applications of 3DE guidance: 3D TOE has been used during catheter-based closure of Fontan fenestrations,[82] ruptured sinus of Valsalva aneurysms,[83] coronary artery fistulas,[84,85] prosthetic valve para-valvar leaks,[86–88] atrial switch baffle leaks or obstruction,[89,90] atrial septum trans–septal puncture,[91] and biventricular pacemaker synchrony assessment and lead placement.[92] Recently, intracardiac echocardiography transducers have been developed with 3D capability in a segment of ~60 × 15° using a 10-French probe. Early work has demonstrated visualization of the atrial and ventricular septums, aortic valve, mitral valve, and atrial appendages for guidance of intervention.[93–95]

Future directions

Miniaturization of 3D TOE probes for use in smaller patients and enhanced automation are likely future developments. The introduction of 3D intracardiac probes will provide an alternative to the TOE approach. The application of fusion imaging of 3D TEE with fluoroscopy, 3D rotational angiography, cardiac MRI, and CT

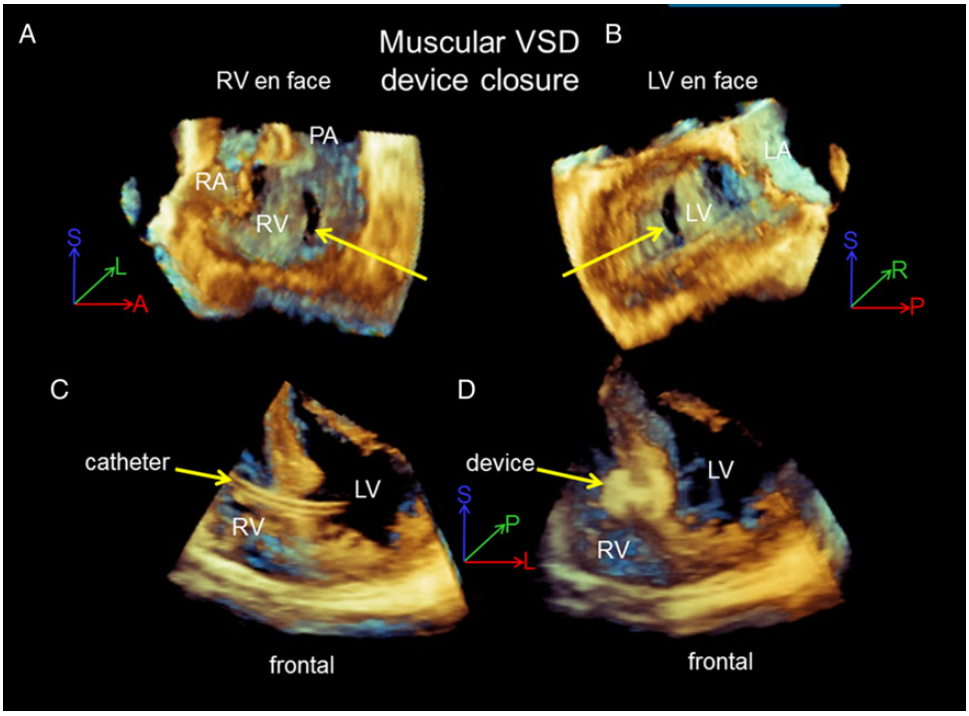

Figure 12 3DE permits en face visualization of the ventricular septal defect to provide information on defect location, size, and adjacent structures. In this example, 3D TOE was used. A muscular defect is seen from the right ventricular aspect (*A*) and LV aspect (*B*). During positioning of catheters (*C*) and device deployment (*D*) 3DE can assist. In each panel of this figure, the ventricular septal defect (VSD) is arrowed. RA, right atrium; LA, left atrium; RV, right ventricle; LV, left ventricle; PA, pulmonary artery; S, superior; L, left; R, right; P, posterior; A, anterior.

angiography is also likely to expand as interventions become more complex.

Recommendations

Use of 3DE to guide catheter-based interventions

3DE is recommended to assist interventional closure of selected ASDs and VSDs, particularly multiple, irregularly shaped, or residual defects.

Real-time 3D imaging is recommended for visualization of catheters, delivery systems, and devices during catheter intervention in CHD.

Use of 3DE to measure defects (either MPR or rendered 3D images) is recommended to assist interventional catheter procedures involving CHD.

Three-dimensional echocardiographic assessment of ventricular volumes and ventricular function

There are many challenges with assessment of the RV and LV in patients with CHD, including abnormal cardiac position, abnormal connections, septal defects, non-contractile patch material, and abnormal loading conditions. These difficulties are additive to generic considerations such as adequate temporal resolution to determine the chamber volume throughout the cardiac cycle with accuracy. Above all, however, in CHD ventricular geometry may be far removed from the normal geometry around which software packages have been designed, so that analysis algorithms may not be valid. Nonetheless, 3DE has been applied in CHD because assessment of cardiac volumes and function are being increasingly used to plan patient management,[54] and subjective assessment is unreliable.[96]

3DE assessment of the right ventricle

Assessment of RV size and function is important in clinical practice, particularly in patients with repaired tetralogy of Fallot (TOF) and other surgical repairs utilizing an RV to pulmonary artery conduit where RV measurements impact on the timing of pulmonary valve replacement. The position of the RV immediately behind the sternum complicates imaging windows, and subcostal imaging may not be adequate beyond the early childhood years. Prominent trabeculations complicate endocardial border delineation, and normal RV geometry is complex with a triangular appearance in the sagittal plane and a crescent shape in the coronal plane. RV inflow and outflow tracts are also located in different imaging planes. All these hinder capturing the RV in its entirety by ultrasound and preclude the use of a simple geometrical formula to calculate volumes and ejection fraction (EF). 3DE has potential advantages for assessment of RV volume because it makes few assumptions about ventricular shape. Three 3DE techniques have been applied to measure RV

Table 4 Published data on estimation of RV volumes by different echocardiographic techniques compared with values derived from magnetic resonance imaging

Echo method and reference	Population	*N*	Feasibility (%)	EDV correlation/ agreement with MRI	ESV correlation with MRI	EF correlation with MRI	Mean difference EDV	Reproducibility (EDV) ICC (%) or limits of agreement (mL)	Test–retest
Method of discs									
Lu *et al.*[98]	Healthy children	20	85	$r = 0.98$	$r = 0.96$	$r = 0.89$	-3.2 ± 7.0 mL	Intra: 2.1 ± 5.3% Inter: 5.4 ± 9.2%	
Renella *et al.*[99]	Varied, including normal and CHD	70	58	–	–	–	–	Intra: −1.9 mL (−5.1 to 1.3) Inter: −2.0 mL (−6.0 to 2.1)	−0.50 (−3.5 to 2.5)
Semi-automated border detection									
Maffessanti *et al.*[100]	Healthy adults	540	94	–	–	–	–	Intraobserver COV 2–8.6% Interobserver COV 7–15%	–
Tamborini *et al.*[101]	Healthy adults	245	94	–	–	–	−10 mL	Intra: 0.6 ± 5.1 Inter: 0.9 ± 20.3	0.2 ± 6.9
Leibundgut *et al.*[102]	Adults with cardiac dysfunction	100	92	$r = 0.84$	$r = 0.83$	$r = 0.72$	−10 mL	Intra: ICC 0.93 Inter: ICC 0.95	
Jenkins *et al.*[103]	Adults with cardiac dysfunction	54	93	$r = 0.6$	$r = 0.55$	$r = 0.78$	-3 ± 10 mL	Intra: $r = 0.94$, 1 ± 3 mL Inter: $r = 0.76$, 0 ± 10	$r = 0.91$, 0 ± 5
Dragulescu *et al.*[104]	Children with CHD	70 (36 vs. MRI)	91	$r = 0.98$	$r = 0.98$	$r = 0.85$	18.2 ± 17.8	Intra: COV 5.4 Inter: 8	
Khoo *et al.*[17]	Children with CHD	54	52	$r = 0.91$	$r = 0.9$	$r = 0.76$	-19.3 ± 6 14	Inter: ICC 0.97, 11.6 ± 7.0	
Grewal *et al.*[105]	Adults with CHD	25		$r = 0.88$	$r = 0.89$		−9%, max 34%	Inter: 10%	
Van der Zwaan *et al.*[106,107]	Adults with CHD	62	81	$r = 0.93$	$r = 0.91$	$r = 0.74$	34 mL LOA −32 to 99	Intra: 1 ± 12 Inter: ±	7%
Iriart *et al.*[108]	Adults with repaired TOF	34	92	$r = 0.99$ ICC = 0.99	$r = 0.98$ ICC = 0.98	$r = 0.86$ ICC = 0.85	18.7 ± 12.2	Inter: 0.4 ± 0.3	
Grapsa *et al.*[109]	Adults normal+PAH	80		$r = 0.75$ −3.7 mL LOA 52.6 mL	$r = 0.74$	−1.3% LOA 12.5		Inter: ICC 0.89	10.6%
Knowledge-based reconstruction									
Dragulescu *et al.*[110]	Children with TOF	30	100	$r = 0.99$	$r = 0.99$	$r = 0.87$	-2.5 ± 3.7 mL	Intra $r = 0.997$ Inter: $r = 0.995$	
Dragulescu *et al.*[104]	Children with TOF (40 vs. MRI)	70	98	$r = 0.99$	$r = 0.99$	$r = 0.94$	6.6 ± 10.7	Intra: COV 3.4 Inter: COV 3.8	

Kutty *et al.*[111]	Adolescents and adults with systemic RV	15	100	$r = 0.80$	$r = 0.82$	$r = 0.86$	−4.3%	Intra: 3.2% Inter: 4.6%	
Single-beat full-volume capture	Population	*N*	Feasibility (%)	EDV correlation/ agreement with MRI	ESV correlation with MRI	EF correlation with MRI	Mean difference EDV	Reproducibility	Test–retest
Zhang *et al.*[112]	adults normal and with cardiac dysfunction	61	96.7	$r = 0.97$ Bias: 2.16 LOA: 15.1	$r = 0.96$ Bias: 2.6 LOA: 15.8	$r = 0.71$ Bias: 0.86 LOA: 16	2	Intra: ICC 0.97 Inter: ICC 0.97	EDV ICC 0.96, mean difference −1.7

EDV, end-diastolic volume; ESV, end-systolic volume; EF, ejection fraction; RV, right ventricle; MRI, magnetic resonance imaging; Intra, intraobserver; Inter, interobserver; Bias, LOA, bias and limits of agreement between two methods assessed by Bland–Altman analysis; ICC, intra-class correlation coefficient.

volumes and EF, namely summation of discs, semi-automated border detection, and knowledge-based reconstruction.

Summation of discs

The semi-automated method of disc summation is conceptually most comparable with MRI analysis and has been validated in children by water displacement[97] and MRI.[98] Feasibility of this method is good in healthy children (*Table 4*), although a recent study in older patients found feasibility in $<60\%$.[99] Although there is excellent correlation with MRI-derived RV volumes, the values from 3DE tend to be lower.[98] The disc summation method retains landmarks which may be abnormally positioned or absent in CHD.[18,113] Unfortunately, summation of disks methodology has been removed from some software packages, thereby removing the closest correlate with MRI.

Semi-automated border detection

This is the most common 3DE method to assess RV volumes and EF. A full-volume 3D data set is acquired and segmented into four-chamber, sagittal, and coronal views (*Figure 13A*). Key RV and LV anatomical landmarks are defined, and end-diastolic and end-systolic contours are manually drawn in each view to construct a dynamic polyhedron model of the RV (*Figure 13A* and *B*). In healthy adults, this methodology is feasible;[101,102] volumes and EF correlate well with MRI, although 3DE underestimates volumes compared with MRI (*Table 4*). Acquisition time is significantly shorter for 3DE than for MRI (~5 vs. 20 min).[17,106] In healthy adults and children, intra- and inter-observer reliability is good[98,101] (*Table 4*) but agreement with MRI worsens in adults with cardiac dysfunction (*Table 4*).[103,109]

In adults after TOF repair, correlation with MRI is good for end-systolic volume (ESV), end-diastolic volume (EDV),[104–106] and EF; however, 3DE produces lower volumes compared with MRI (*Table 4*).[105] Individual differences between the techniques can be substantial, and the limits of agreement are wide. The disparity between 3DE and MRI becomes larger in the severely dilated RV where there are particular difficulties in the incorporation of the whole RV, particularly the RV outflow tract in a single volume.[105,106,108,114] Intraobserver, interobserver, and test–retest reliability varies among studies, but is generally acceptable (*Table 4*).[104,106,107] In children with hypoplastic left heart syndrome, 3DE has good reproducibility during serial follow-up.[115] However, 3DE measurements are a mean 30% lower than MRI with larger differences in smaller patients, so the techniques cannot be used interchangeably.[116]

Most published RV data utilize full-volume 3DE datasets acquired over several cardiac cycles and normal adult ranges.[100] Recently, 3DE RV volumes and function has been studied using single-beat acquisition in adults.[112] Feasibility was very good (96.7%) as were correlation and agreement with MRI; however, the reduced temporal resolution remains a concern for application to younger patients with higher heart rates.

Knowledge-based 3D reconstruction

Knowledge-based 3D reconstruction evaluates 3D RV volumes from a series of 2DE images localized using a magnetic tracking system (*Figure 14*).[117] RV anatomic landmarks are identified on the

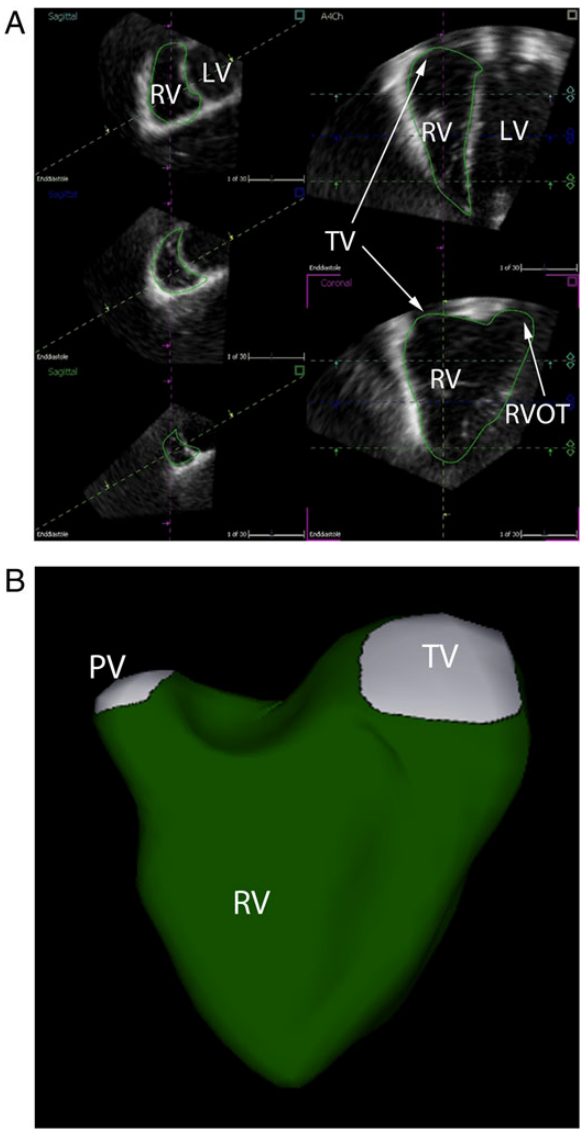

Figure 13 Measurement of right ventricular volume by transthoracic 3DE. (*A*) Analysis packages designed specifically for the right ventricle are based on user defined reference points and semi-automated tracking of the endocardial border. The green lines show the endocardial border in reference planes including sagittal (left panels), apical projection (upper right panel), and angled coronal planes (lower right panel). (*B*) Once the user defined planes have been set, a representative model of the right ventricle can be produced, the boundaries of which define EDV and ESV. LV, left ventricle; RV, right ventricle; TV, tricuspid valve; RVOT, right ventricular outflow tract.

images, which are processed over the Internet using a reference lesion-specific MRI database. This technique has been validated against MRI in children after TOF repair.[110,118] Bias, intra- and inter-observer reliability were good, and knowledge-based 3D reconstruction was slightly better than semi-automated border detection method in this regard. In adults with a systemic RV[111,119] and

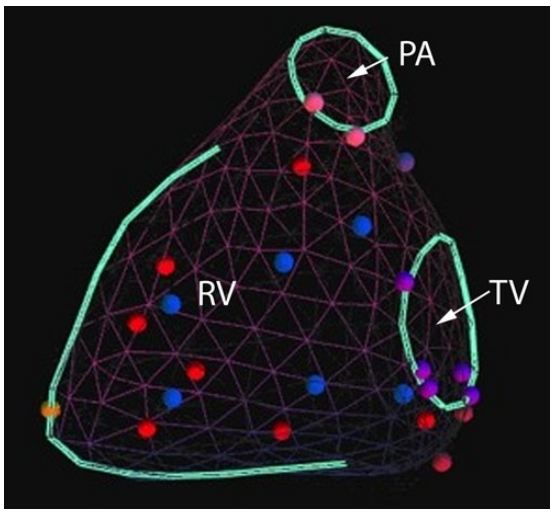

Figure 14 RV volume calculated using knowledge-based reconstruction. This technique is based on placing reference points on transthoracic 2DE images of different projections of the right ventricle, using a defined protocol and a tracked probe. Each of the points (red, blue, purple, pink, and orange) represents a specific reference point. The full volume is reconstructed by uploading the information to a server which is linked to a disease specific atlas to complete the contouring and volume generation. TV, tricuspid valve; RV, right ventricle; PA, pulmonary artery.

pulmonary arterial hypertension, values have shown good agreement with MRI.[120,121] Limitations of the knowledge-based technique include the necessity for a tracked ultrasound transducer and for the patient to remain still throughout the study.

3DE assessment of the LV

Reliable assessment of LV volume and function is important in patients with CHD. 2DE has important limitations in CHD because, in contrast to 3DE, it makes assumptions of LV shape which are frequently invalid in this population. Thus, 3DE can contribute significantly to the assessment of LV volumes, function, and mass.

Analysis methods

The 3DE dataset is obtained from an apical or modified transducer position to include the entire LV volume, which is usually feasible except when the LV is severely dilated. Current software tracks the endocardium of the LV throughout the cardiac cycle and therefore depends on adequate image quality and acoustic windows. Vendors typically display reference planes used to define the endocardial border (*Figure 15*) as well as the 'shell' of the LV itself (*Figure 16*). Current tracking algorithms involve user definition of key reference points followed by semi-automated tracking of the endocardium, but the operator can manually override the initial automated selection of the endocardial border.[122]

Despite difficult endocardial delineation and heterogeneous LV shapes, accurate determination of LV volume and function by 3DE has been reported in adults and children with CHD using MRI as the

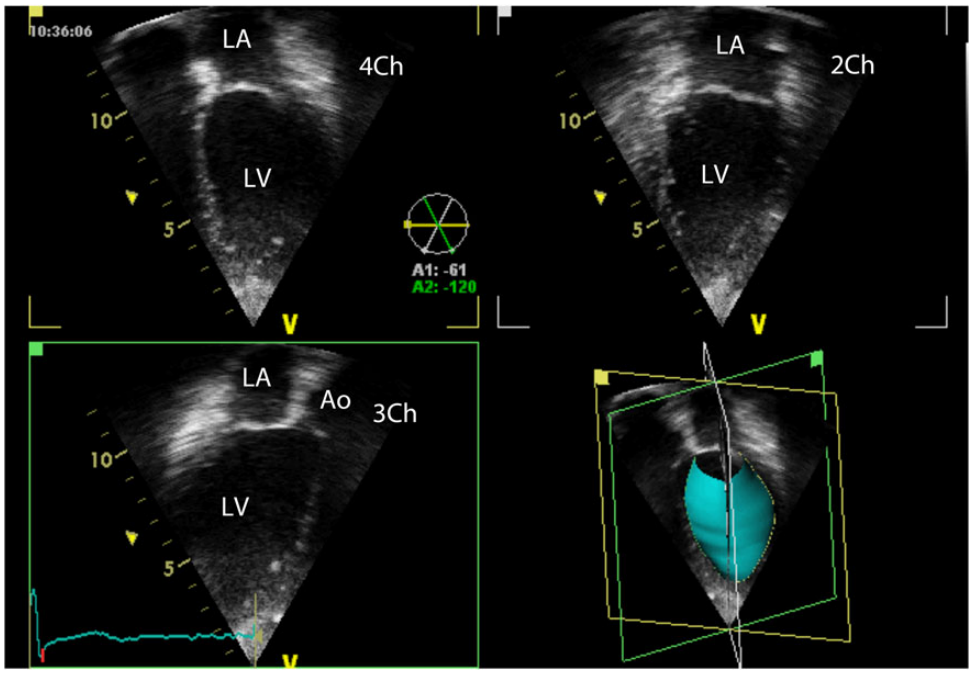

Figure 15 'Triplane' view of the left ventricle. This view permits visualization of the apical four-chamber, two-chamber, and three-chamber views as well as the volume defined by the endocardial border of the three reference planes. LA, left atrium; LV, left ventricle; Ao, aorta.

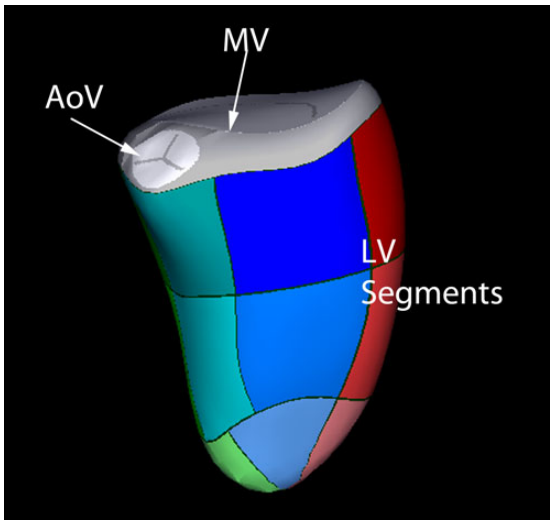

Figure 16 Segmental view of LV. 3DE can be used to assess LV volume, ejection fraction, and synchrony based on tracking of the endocardial border of the ventricle. A standard segmentation of the ventricle is used to colour encode the basal, mid, and apical segments. Most software algorithms assume a central axis from the mitral valve to the LV apex so that this type of analysis has not been validated for ventricles of more complex shape. AoV, aortic valve; MV, mitral valve.

gold standard. Potential errors can still occur in children who have higher heart rates and smaller LV volumes compared with adults, which is offset by superior image quality. 3DE compares favourably with MRI but has a bias to producing lower LV EDV and ESV compared with MRI in patients with CHD in a meta-analysis of 3055 subjects from 95 studies.[123] The repeatability of 3DE for estimation of LV volume is good and supports its role for serial follow-up, although the values are not interchangeable with those obtained by MRI in the CHD population. Validation studies in children and adults with CHD are listed in *Table 5*.[98,113,125,126,129,130] 3DE is more accurate and reproducible than either M-mode or 2D Simpson's biplane method and is as feasible as 2DE in children.[127,131] These findings have also been validated in neonates and infants where 3DE has compared favourably with MRI even when LV volumes are small and heart rates are high.[113]

LV mass

3DE has been used to assess LV mass in children and compared with both 2DE and M-mode.[132] In younger patients, M-mode has remained the most widespread technique because of the availability of normal paediatric ranges.[133,134] 3DE methods are based on calculating the endo- and epicardial volumes, which are subtracted to compute the mass. 3DE values correlate well with MRI, with low inter- and intraobserver variability[135] but the limits of agreement remain wide.[98,113,125,129] Therefore, the clinical application of 3DE for LV mass calculation in patients with CHD remains to be established.

Table 5 Results of published data comparing 3DE and MRI in patients with CHD and children

Echocardiographic method	Population	*n*	Feasibility (%)	EDV correlation/ agreement with MRI	ESV correlation with MRI	EF correlation with MRI	LV mass	Mean difference EDV	Reproducibility (EDV)
Disk summation									
Altman *et al.*[124]	Children and adults with functional single ventricle	12		$r = 0.98$	$r = 0.98$	Mean diff. 4.4 ± 10%	Mean diff. 5.8 ± 19 g	−2.9 ± 8.1 mL	
Soriano *et al.*[18]	Children with functional single ventricle	29	93	$r = 0.96$	$r = 0.94$	$r = 0.64$	$r = 0.84$	−3.8 ± 13 mL	Intra: ICC 0.99 Inter: ICC 0.97
Friedberg *et al.*[113]	Children with CHD	35		$r = 0.96$	$r = 0.90$	$r = 0.75$	$r = 0.93$	−0.49 ± 2.6 mL	Intra: ICC 0.98 Inter: ICC 0.97
Semi-automated border detection									
Bu *et al.*[125]	Healthy children	19		$r = 0.97$	$r = 0.97$	$r = 0.86$	$r = 0.97$	−6.83 ± 9.66 mL	Intra: 2.9 ± 3.0% Inter: 7 ± 5%
Van den Bosch[41,95]	Adults with CHD	32,	22	91	$r = 0.95$	$r = 0.97$	$r = 0.88$	$r = 0.94$	
Intra: ICC 0.96 Inter: ICC 0.92 Inter: ICC 0.99									
Riehle, *et al.*[126]	Children and young adults with CHD	12		$r = 0.99$	$r = 0.93$	$r = 0.69$		−4.11 ± 5.16 mL	Intra: 0.4 ± 5.3% Inter: 3.3 ± 4.3%
Lu *et al.*[127]	Healthy children	19		$r = 0.96$	$r = 0.93$	$r = 0.88$	$r = 0.98$	−6.93 ± 9.71 mL	Intra: 1.0 ± 5.2% Inter: 3.2 ± 3.8%
Laser *et al.*[128]	Healthy children and children with TOF	49		$r = 0.95$	$r = 0.91$				Intra: ICC 0.99 Inter: ICC 0.98
Poutanen *et al.*[129]	Healthy children	30		$r = 0.80$	$r = 0.88$	$r = 0.20$	$r = 0.81$	−4.0 ± 19.6 mL	Intra:ICC 0.92 Bias −1.0 ± 13.0 Inter:ICC 0.83 bias 4.7 ± 17.6
Ylanen *et al.*[130]	Children with normal cardiac anatomy	71		$r = 0.88$	$r = 0.83$	$r = 0.12$		−24 ± 32 mL	Intra: ICC 0.98 Inter: ICC 0.88

EDV, end-diastolic volume; ESV, end-systolic volume; EF, ejection fraction; LV, left ventricle; MRI, magnetic resonance imaging; Intra, intraobserver; Inter, interobserver; Bias, LOA, bias and limits of agreement between two methods assessed by Bland Altman analysis; ICC, intra-class correlation coefficient.

3DE assessment of LV intraventricular dyssynchrony

The capability of 3DE to capture the entire LV volume offers the opportunity to assess global and regional LV function (*Figure 16*). Ventricular dyssynchrony is expressed as the standard deviation of the time taken for segments to reach their minimum systolic volume, indexed to the cardiac cycle length [Systolic Dyssynchrony Index (SDI)].[136] Normal values of SDI in children and adolescents are lower than the adult population.[137,138] 3DE estimates of LV dyssynchrony appear to be most repeatable if a 16-segment model is used as opposed to 12 or 6 segment models.[139] 3DE has been used to demonstrate increased LV dyssynchrony in children with Kawasaki disease[140] as well as dilated cardiomyopathy where the 16-segment SDI correlated negatively with 3DE EF and 2DE fractional shortening.[141] 3DE has also demonstrated LV dyssynchrony in patients with tricuspid atresia after Fontan palliation[142] and a high incidence of LV regional wall motion abnormalities in CHD patients.[143] Current software packages define abnormal wall motion with respect to the central LV axis which has limitations for some CHD patients with an LV of unusual shape. Further difficulties in measurement of dyssynchrony occur where LV function is poor due to difficulties in accurate determination of the point of minimum systolic volume in segments where such curves are of low amplitude.[144] Caution is required when using 3DE as a modality to quantify electromechanical dyssynchrony in CHD in the absence of a significant body of evidence.

3D wall tracking of the left ventricle

Recent advances in 3D wall tracking have allowed for assessment of myocardial deformation in three dimensions from a single volume of the LV (*Figure 17*). The 3D technique has a potential advantage over 2D strain in that loss of tracking due to through plane motion can be avoided.[145] This permits a semi-automated analysis of longitudinal, radial, circumferential, and 3D strain from a single volume. In addition, LV volume, EF, and LV twist and torsion can be computed from the same volume. The major limitations of this technique remain temporal resolution and feasibility of incorporating the entire LV. Recent publications have reported normal values in children and adolescents,[146,147] but this currently remains a research tool, and the place of such analysis in the management of patients with CHD remains to be established.

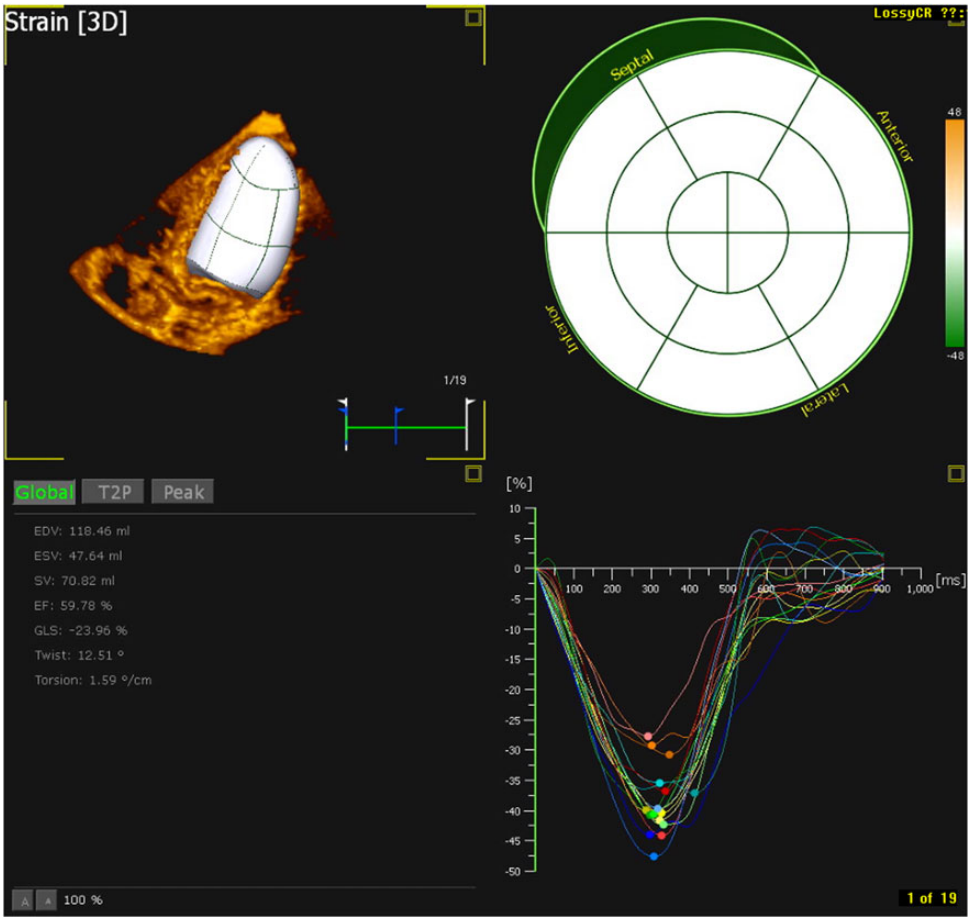

Figure 17 3D deformation analysis by wall tracking. Some software uses the 3D volume to track the myocardium of the left ventricle rather than simply the endocardial border. This permits analysis of deformation, twist and torsion of the whole of the left ventricle from a single volume. A limitation of the technique is that the temporal resolution is lower than 2DE.

Assessment of the functional single ventricle

Ventricular dysfunction is an important long-term complication in patients with functionally single ventricle circulation. 3DE based on disc summation appears feasible and compares favourably with MRI.[18,124] Semi-automated border detection has been applied to the serial assessment of RV volumes and EF in hypoplastic left heart syndrome[115] but with systematic underestimation of RV volume compared with MRI.[116] The differences may reflect the tendency for semiautomatic methods to skim the surface of trabeculations, geometric limitations, and failure to include the entire ventricle by 3DE.

Future directions

Technical solutions such as the fusion of multiple 3DE volumes may assist in acquiring the entire ventricular cavity for the purposes of RV functional assessment.[148] The availability of the semi-automated method of disks algorithm for RV volumetry is desirable, as is the availability of analysis software that is purpose-designed, including the facility to landmark structures in normal and abnormal hearts. The availability of large studies to define normal RV and LV volumes and mass across a wide range of body size would enable these measurements to replace 2D measurements in clinical practice. The availability of automated, reproducible algorithms that provide for geometry-independent volumetric analysis of congenitally abnormal ventricles would enhance application in serial follow-up.

Recommendations

Assessment of ventricular volumes and function in CHD

Measurement of ventricular volumes and EF by 3DE is highly repeatable.

3DE has a systematic bias to produce lower values of volume than MRI so that measurements should not be used interchangeably.

Current implementation into clinical practice is hampered by a paucity of normal data from infancy through to adulthood.

Software developed for the normal LV or RV should not be applied to patients with congenitally abnormal ventricles without being validated.

The semi-automated summation of disc method is the least constrained by geometry and should be included with post-processing software particularly for ventricles of abnormal morphology.

3D echocardiographic assessment of atrioventricular and arterial valve function in CHD

3DE assessment of AV valves in CHD is one of the most frequently used applications of the technology in a clinical setting.[149,150] 3DE provides comprehensive information on AV valve size, morphology, and motion. The application of 3D colour flow Doppler can be used to visualize regions of AV valve regurgitation including the size, shape, and number of regurgitant orifices.

The AV valves

Assessment of AV valve anatomy

3DE assessment of AV valves in CHD is driven by the need for better visualization and understanding of the mechanism of the valve regurgitation during surgical planning. AV valve function is a complex interaction of atrial contraction;[151] annular shape, contraction, and motion;[152,153] leaflet size, shape[154,155] and the changes in its tensor strength,[156,157] chordal length and tension as well as papillary muscle contraction and position.[158,159] Ventricular coordination and contraction[160,161] also impact on AV valve function. 3DE assessment focuses on the valve annulus, leaflets, chords and papillary muscles, as these are the AV valve components that can be manipulated or repaired by current surgical techniques. Although quantitative 3DE assessment of the AV valve in CHD has been reported for AV septal defects[159,162] and tricuspid valves in hypoplastic left heart syndrome,[158,163] it is still not part of routine clinical practice. Commercially available quantitation software frequently assumes normal AV valve morphology and acquired disease, making it less valid for use in CHD. Currently, the assessment of AV valve regurgitation by 3DE remains largely qualitative[41] and is tailored to the individual valve anatomy. There are no data on the impact of 3DE on clinical outcomes in CHD but the technique may impact on the surgical approach.[164]

Quantitation of AV valve regurgitation

Assessment of AV valve regurgitation severity by 2DE has been demonstrated to guide management in the adult population[165] despite significant interobserver variation.[166] 2DE guidelines have been produced for quantitative assessment of valvular regurgitation in adults[167,168] but not children.[24] Poor reproducibility and accuracy result from morphologically abnormal valves, complex regurgitant jet morphology with an elliptical or linear regurgitant orifice and multiple jets, and effective regurgitant orifice area (EROA) calculation has not demonstrated major benefit compared with qualitative assessment.[169–171] EROA reference values relative to patient or valve size are not available, which is a significant limitation in the interpretation of results in growing patients with congenitally abnormal valves. 3DE methods analogous to MRI for estimation of valve regurgitation are encouraging[172–174] but are limited by the requirement of no significant interventricular shunts. 3DE quantification of AV valve regurgitation *vena contracta* area in CHD is a promising approach, is relatively simple to measure, and is available on most 3DE navigation software. After acquiring a 3DE colour mapping dataset, the clinician can navigate within the MPR mode to directly measure the *vena contracta* area perpendicular to the regurgitant jet. Multiple validation studies in the adult population have shown strong correlation between 3DE *vena contracta* area of mitral regurgitation and MRI calculated EROA and regurgitation fraction with high reproducibility.[175] Further validation in paediatric and CHD patients is still required.

Quantitation of aortic and pulmonary valve stenosis and regurgitation by 3DE

The aortic valve

The central role of echocardiography in the investigation of aortic valve disease is well established in both paediatric/congenital and

adult practice.[24,176,177] As previously discussed, 3DE can define valve morphology and estimate LV volume and mass. Doppler-derived pressure drop across valves is flow dependent, and accurate measurement of effective aortic valve orifice area is clinically important. This is particularly important in children where use of the continuity equation has not been recommended because of the potential for measurement error.[24] MPR images can be adjusted to ensure an *en face* orientation to assist in direct measurement of the effective aortic valve area in children with aortic valve stenosis.[21,178] 'Cut off' values of area in children cannot be used because this is impacted by the size of the aortic valve, which is in turn related to the size of the child. Previous published work has addressed the normal aortic valve area across a wide age and size range,[179] but this normative data used a rotational probe rather than current real-time 3DE techniques. Thus, it is feasible to planimeter the effective aortic valve area in the paediatric population, but data on the impact of such measurements on timing of intervention or prognosis is lacking.

Echocardiographic quantification of aortic valve regurgitation has been addressed in several documents,[24,176,177] and standard indices include LV dimensions, regurgitant jet or *vena contracta* diameter, and diastolic reversal of flow in the aorta. Recent adult work has used 3DE colour estimation of the size of the 3DE-derived *vena contracta* against 2DE and MRI with encouraging results.[180,181] This technique has not been validated in paediatric or congenital populations. Surgical planning for patients with aortic valve disease involves quantitation of aortic root size, with evidence of improved accuracy using 3DE in children[51] and validation of automated 3DE in adults.[182]

The pulmonary valve

Assessment of pulmonary valve stenosis in children and adults with CHD is normally based on Doppler-derived pressure drop across the valve.[24] Obtaining an *en face* image of the pulmonary valve by 2DE may be challenging, which hampers definitions of stenosis based on effective pulmonary valve orifice area. 3DE may assist in projecting the pulmonary valve *en face* either by real-time 3DE, by cropping a multi-beat full volume, or by utilization of cross-plane techniques. Pulmonary regurgitation is an important complication of many patients with CHD, particularly those with repaired TOF or with conduits from the RV to the pulmonary artery. Recent publications[54,114,183] emphasize the importance of quantifying the size and function of the RV by 3DE. The estimation of pulmonary regurgitation by 3DE remains semiquantitative; although there are published data using 3DE to measure EROA,[184] it has not been adopted into CHD practice and has not been validated against cardiac MRI.

Recommendations

Atrioventricular valves

The use of 3DE to visualize AV valves, papillary muscles, and chordal support is recommended to assist surgical planning.

3DE assessment of the location, size, shape, and number of regurgitant jets and orifice area is recommended.

Measurement of EROA needs to be validated in children and adolescents and in a wide range of valve pathology before its measurement can be recommended to quantify AV valve regurgitation and impact timing of valve repair or replacement.

Post-processing software for AV anatomy and valve function needs to be used with caution as it may assume normal valve anatomy.

Arterial valves

3DE is recommended to assess the morphology of the aortic and pulmonary valves.

3DE is recommended for the measurement of annulus, root and effective orifice area measurement.

3DE colour flow Doppler measurements remain to be validated as a means of quantifying arterial valve regurgitation.

Training in three-dimensional echocardiography

Requirements and recommendations for training have been an integral part of position statements and guidelines for echocardiography in CHD.[185–187] No such proposals have been produced for 3DE of CHD, and the European certification process for echocardiography of CHD does not currently include 3DE at all.[188] Training and education play a critical role in increasing the utility of 3DE, particularly in terms of its ability to improve outcomes.[189] There is no question that the adoption of 3DE into clinical routine has a learning curve and demands specific training.

Machines and transducers for 3DE are similar to those for 2DE. There are some fundamental differences in the approach to learning 2DE vs. 3DE. In 2DE, the only image that can be interpreted is the acquired 2D image. A central component of training is the appropriate acquisition of images in planes that are largely predefined. In contrast, 3DE involves acquisition of a 3D dataset with extensive potential for post-processing. Training in 3DE must involve methods to develop and improve the ability to acquire optimal 3DE datasets and to post process the sonographic volumetric datasets to show cardiac morphology or quantify ventricular function. Recognition and evaluation of *en face* views of valves and septums must be learned as well as other details of complex intracardiac anatomy uniquely available through 3DE. While these structures and views are familiar to surgeons, pathologists, and others who have an implicit understanding of cardiac anatomy, they pose a challenge to those who do not have such a frame of reference. One approach to helping bridge this gap has been the development of educational programmes and publications that include side-by-side depiction of pathology specimen photographs and 3DE images for a wide range of CHD.[60]

Training in acquisition has, of necessity, involved live scanning of subjects in a classroom or clinical setting. Although it provides an authentic learning experience, this mode of learning has practical limitations, including class size, availability of cooperative subjects with a wide spectrum of disease states, busy clinical settings, and issues related to privacy. Over the past few years, simulators to teach 2D TOE and TTE have become available but 3DE simulators are lacking.[190,191]

Training in post-processing has primarily occurred in the format of workshops involving manipulation of datasets from a wide range of pathologies.[192] This type of training requires high-quality 3DE datasets of a variety of CHD, a large number of portable computers

and vendor-specific software. One of the challenges of 3DE training has been the high frequency of modifications of the user interface for both acquisition and post-processing.[189] While this is to be expected in the evolution of the modality, frequent changes of user interface may discourage adoption of 3DE. Stability of the user interface and consistency between manufacturers would help greatly in developing robust tools for training.

A further consideration is the wide variability in the use of 3DE between centres and adoption of 3DE within certification and training programmes. There are no specific guidelines for education related to 3DE in the published North American guidelines for core fellowship training in paediatric cardiology,[185] and the revised guidelines include only vague references to 3DE experience for advanced fellowship training in non-invasive imaging.[193] 3DE is not a current component of the European certification process in echocardiography of CHD. The absence of specific training standards for 3DE has resulted from the absence of guidelines and standards for the performance and interpretation of 3DE studies. This document should provide a framework for more structured 3DE training in the future.

With respect to what form such training should take, attendance at a formal training course in acquisition and post-processing of 3DE is essential to understand different 3D modalities and post-processing software. Sonographers and cardiologists in training should continue to establish their core skills in 2DE according to established training programmes. For trainees subspecializing in echocardiographic imaging, many should be able to gain the further experience in data acquisition and post-processing within their unit, provided 3DE is being widely used. Assessment should be competence based but acquisition of and post-processing of at least 50 volumes (mixed TTE/TOE) of different forms of CHD would seem reasonable. Competence should include assessment of cardiac morphology as well as quantitation of LV volume and EF. If a centre does not offer exposure to a high volume of 3DE then a period of training of 3–6 months at a high-volume centre would be appropriate. For the advanced practitioner, application of 3DE in the catheterization laboratory and during surgery requires advanced and rapid acquisition and post-processing skills and will generally require more experience and training than that outlined above. Application of 3DE to the RV or abnormally shaped ventricles will also require further experience and training. Trainers in 3D echocardiography will be drawn from cardiologists with many years of experience of acquisition and post-processing of structure and function using 3D echocardiography. It is hoped that the recommendations in this document, for examples those relating to image orientation, may assist in development of structured programs both for trainees and trainers.

Future directions

Echocardiography simulators should be modified to include training in 3DE acquisition. The development of a comprehensive simulation-based educational resource would require a large library of 3DE datasets encompassing a wide range of pathologic states. Training in post-processing should involve web-based access to 3DE analytic software in conjunction with an online library of 3DE datasets of various CHD lesions. In order to develop such libraries, anonymization tools for Digital Imaging and Communications in Medicine (DICOM) datasets including removal of both DICOM headers and patient data displayed in the image are essential.

Recommendations

Training in 3DE

Training in 3DE should be an integral part of the training of the congenital echocardiographer. This should include the indications for and added value of 3DE in surgical and interventional planning and guidance.

Training should include 3DE dataset acquisition and post-processing to demonstrate competence in assessment of cardiac morphology and quantification of cardiac function.

Operators should learn to recognize and evaluate cardiac views which are uniquely feasible by 3DE including *en face* views of valves and septums.

A degree of consistency of the user interface and uniformity of terminology between manufacturers would help greatly in developing robust non-proprietary tools for training.

Advances in three-dimensional echocardiography

While the past decade has brought exciting advances to the fore in 3DE, there are many aspects that would benefit from improvements in technology that are tailored to the patient with CHD. We look forward to advances in transducer design and computer post-processing as well as research into novel methodologies, such as frame reordering[194] and image compounding,[148,195,196] which can achieve benefits in terms of field of view, endocardial border definition, enhanced temporal resolution, and intraventricular flow. Advances in 3D printing[197,198] and in holographic displays promise the ability to view, understand, and utilize 3DE data better in clinical practice.

Novel measurements of ventricular volumes, 3D deformation, valvar morphology, valvar function, and flows should be validated, automated, and lead to publication of robust normal ranges across a wide range of ages and body size. These enhancements should not be limited to left heart structures but need to be comprehensive to include the right heart and congenitally abnormal ventricles and valves. All of these measures need to undergo robust assessment of their repeatability and accuracy vs. other imaging techniques.

The assessment of the impact of 3DE techniques on patient outcome remains a challenge. Many current 3D techniques have been adopted in an *ad hoc* manner to address specific clinical challenges such as surgical repair of CHD or guidance of interventional procedures but without robust analysis of impact on outcome. Quantitation of ventricular volumes, myocardial deformation, and cardiac function by 3DE needs to stimulate research studies that demonstrate whether or not 3DE measures can be used as surrogates for outcome.

The technical advances and increased use of 3DE techniques in clinical practice will place greater emphasis on improved methods for training and education in 3DE. This needs to be matched at the research and development stage by improvements in the software interface for acquisition and analysis of 3DE including, where

appropriate, increased automation to improve workflow and reduce observer error.

Reviewers

This document was reviewed by members of the 2014–2016 EACVI Scientific Documents Committee, and external reviewers.

EACVI reviewers included: Prof. Gilbert Habib, Prof. Thor Edvardsen, Dr. Vittoria Delgado, Prof. Erwan Donal, Dr. Denisa Muraru, Associate Professor Kristina Haugaa, Dr. Raphael Rosenhek, Dr. José Ribeiro, Dr. Xavier Iriart.

This document was reviewed by members of the 2015–2016 ASE Guidelines & Standards Committee, the 2015–2016 ASE Board of Directors, and external reviewers.

ASE reviewers included Deborah A. Agler, RCT, RDCS, FASE, Federico M. Asch, MD, FASE, Merri L. Bremer, EdD, RN, EDCS, ACS, FASE, Benjamin Byrd, MD, FASE, Hollie D. Carron, RDCS, FASE, Frederick C. Cobey, MD, FASE, Meryl Cohen, MD, FASE, Patrick Collier, MD, PhD, FASE, Mary Corretti, MD, FASE, Adam Dorfman, MD, FASE, Benjamin Eidem, MD, FASE, Fadia Makarem Ezzeddine, RT, RCS, FASE, Craig Fleishman, MD, FASE, Neal Gerstein, MD, FASE, Yvonne E. Gilliland, MD, FASE, Lanqi Hua, RDCS, FASE, Allan L. Klein, MD, FASE, Joe R. Kreeger, ACS, RCCS, RDCS, FASE, Roberto M. Lang, MD, FASE, Stephen H. Little, MD, FASE, Sunil Mankad, MD, FASE, Rick Meece, RDCS, RCS, RCIS, FASE, Tasneem Naqvi, MD, FASE, Maryellen H. Orsinelli, RN, RDCS, FASE, Andy Pellett, PhD, RCS, RDCS, FASE, Patricia A. Pellikka, MD, FASE, Michael Quartermain, MD, FASE, Vera H. Rigolin, MD, FASE, Brad J. Roberts, ACS, RCS, FASE, Vandana Sachdev, MD, FASE, Anita Sadeghpour, MD, FASE, Elaine Shea, ACS, RCS, RCCS, FASE, Roman M. Sniecinski, MD, FASE, Raymond F. Stainback, MD, FASE, Cynthia Taub, MD, FASE, Neil J. Weissman, MD, FASE, Susan E. Wiegers, MD, FASE.

Notice and disclaimer: This report is made available by EACVI and ASE as a courtesy reference source for members. This report contains recommendations only and should not be used as the sole basis to make medical practice decisions or for disciplinary action against any employee. The statements and recommendations contained in this report are primarily based on the opinions of experts, rather than on scientifically verified data. EACVI and ASE make no express or implied warranties regarding the completeness or accuracy of the information in this report, including the warranty of merchantability or fitness for a particular purpose. In no event shall EACVI or ASE be liable to you, your patients, or any other third parties for any decision made or action taken by you or such other parties in reliance on this information. Nor does your use of this information constitute the offering of medical advice by EACVI/ASE or create any physician–patient relationship between EACVI/ASE and your patients or anyone else.

Supplementary data

Supplementary data are available at *European Heart Journal – Cardiovascular Imaging* online.

Conflict of interest: none declared

References

1. Hung J, Lang R, Flachskampf F, Shernan SK, McCulloch ML, Adams DB *et al.* 3D echocardiography: a review of the current status and future directions. *J Am Soc Echocardiogr* 2007;**20**:213–33.
2. Lang RM, Badano LP, Tsang W, Adams DH, Agricola E, Buck T *et al.* EAE/ASE recommendations for image acquisition and display using three-dimensional echocardiography. *Eur Heart J Cardiovasc Imaging* 2012;**13**:1–46.
3. Dekker DL, Piziali RL, Dong E. A system for ultrasonically imaging the human heart in three dimensions. *Comput Biomed Res* 1974;**7**:544–53.
4. von Ramm OT, Smith SW. Real time volumetric ultrasound imaging system. *J Digit Imaging* 1990;**3**:261–6.
5. Sheikh K, Smith SW, von Ramm O, Kisslo J. Real-time, three-dimensional echocardiography: feasibility and initial use. *Echocardiography* 1991;**8**:119–25.
6. Simpson JM. Real-time three-dimensional echocardiography of congenital heart disease using a high frequency paediatric matrix transducer. *Eur J Echocardiogr* 2008;**9**:222–4.
7. Acar P, Abadir S, Paranon S, Latcu G, Grosjean J, Dulac Y. Live 3D echocardiography with the pediatric matrix probe. *Echocardiography* 2007;**24**:750–5.
8. Sugeng L, Shernan SK, Salgo IS, Weinert L, Shook D, Raman J *et al.* Live 3-dimensional transesophageal echocardiography. Initial experience using the fully-sampled matrix array probe. *J Am Coll Cardiol* 2008;**52**:446–9.
9. Rawlins DB, Austin C, Simpson JM. Live three-dimensional paediatric intraoperative epicardial echocardiography as a guide to surgical repair of atrioventricular valves. *Cardiol Young* 2006;**16**:34–9.
10. McGhie JS, Vletter WB, de Groot-de Laat LE, Ren B, Frowijn R, van den Bosch AE *et al.* Contributions of simultaneous multiplane echocardiographic imaging in daily clinical practice. *Echocardiography* 2014;**31**:245–54.
11. McGhie JS, van den Bosch AE, Haarman MG, Ren B, Roos-Hesselink JW, Witsenburg M *et al.* Characterization of atrial septal defect by simultaneous multiplane two-dimensional echocardiography. *Eur Heart J Cardiovasc Imaging* 2014;**15**:1145–51.
12. Kutty S, Colen TM, Smallhorn JF. Three-dimensional echocardiography in the assessment of congenital mitral valve disease. *J Am Soc Echocardiogr* 2014;**27**:142–54.
13. Faletra FF, Ramamurthi A, Dequarti MC, Leo LA, Moccetti T, Pandian N. Artifacts in three-dimensional transesophageal echocardiography. *J Am Soc Echocardiogr* 2014;**27**:453–62.
14. Lang RM, Badano LP, Tsang W, Adams DH, Agricola E, Buck T *et al.* EAE/ASE recommendations for image acquisition and display using three-dimensional echocardiography. *J Am Soc Echocardiogr* 2012;**25**:3–46.
15. Fenster A, Parraga G, Bax J. Three-dimensional ultrasound scanning. *Interface Focus* 2011;**1**:503–19.
16. Pandian NG, Roelandt J, Nanda NC, Sugeng L, Cao QL, Azevedo J *et al.* Dynamic three-dimensional echocardiography: methods and clinical potential. *Echocardiography* 1994;**11**:237–59.
17. Khoo NS, Young A, Occleshaw C, Cowan B, Zeng ISL, Gentles TL. Assessments of right ventricular volume and function using three-dimensional echocardiography in older children and adults with congenital heart disease: comparison with cardiac magnetic resonance imaging. *J Am Soc Echocardiogr* 2009;**22**:1279–88.
18. Soriano BD, Hoch M, Ithuralde A, Geva T, Powell AJ, Kussman BD *et al.* Matrix-array 3-dimensional echocardiographic assessment of volumes, mass, and ejection fraction in young pediatric patients with a functional single ventricle: a comparison study with cardiac magnetic resonance. *Circulation* 2008;**117**:1842–8.
19. Bharucha T, Ho SY, Vettukattil JJ. Multiplanar review analysis of three-dimensional echocardiographic datasets gives new insights into the morphology of subaortic stenosis. *Eur J Echocardiogr* 2008;**9**:614–20.
20. Bharucha T, Sivaprakasam MC, Roman KS, Vettukattil JJ. A multiplanar three dimensional echocardiographic study of mitral valvar annular function in children with normal and regurgitant valves. *Cardiol Young* 2008;**18**:379–85.
21. Bharucha T, Fernandes F, Slorach C, Mertens L, Friedberg MK. Measurement of effective aortic valve area using three-dimensional echocardiography in children undergoing aortic balloon valvuloplasty for aortic stenosis. *Echocardiography* 2012;**29**:484–91.
22. Lai WW, Geva T, Shirali GS, Frommelt PC, Humes RA, Brook MM *et al.* Guidelines and standards for performance of a pediatric echocardiogram: a report from the Task Force of the Pediatric Council of the American Society of Echocardiography. *J Am Soc Echocardiogr* 2006;**19**:1413–30.
23. Ayres NA, Miller-Hance W, Fyfe DA, Stevenson JG, Sahn DJ, Young LT *et al.* Indications and guidelines for performance of transesophageal echocardiography in the patient with pediatric acquired or congenital heart disease: report from the task force of the Pediatric Council of the American Society of Echocardiography. *J Am Soc Echocardiogr* 2005;**18**:91–8.
24. Lopez L, Colan SD, Frommelt PC, Ensing GJ, Kendall K, Younoszai AK *et al.* Recommendations for quantification methods during the performance of a pediatric echocardiogram: a report from the Pediatric Measurements Writing Group of the

American Society of Echocardiography Pediatric and Congenital Heart Disease Council. *J Am Soc Echocardiogr* 2010;**23**:465–95.
25. Nanda NC, Kisslo J, Lang R, Pandian N, Marwick T, Shirali G *et al.* Examination protocol for three-dimensional echocardiography. *Echocardiography* 2004;**21**: 763–8.
26. Anderson RH, Razavi R, Taylor AM. Cardiac anatomy revisited. *J Anat* 2004;**205**: 159–77.
27. Simpson J, Miller O, Bell A, Bellsham-Revell H, McGhie J, Meijboom F. Image orientation for three-dimensional echocardiography of congenital heart disease. *Int J Cardiovasc Imaging* 2012;**28**:743–53.
28. Pushparajah K, Miller OI, Simpson JM. 3D echocardiography of the atrial septum: anatomical features and landmarks for the echocardiographer. *JACC Cardiovasc Imaging* 2010;**3**:981–4.
29. Pushparajah K, Barlow A, Tran V-H, Miller OI, Zidere V, Vaidyanathan B *et al.* A systematic three-dimensional echocardiographic approach to assist surgical planning in double outlet right ventricle. *Echocardiography* 2013;**30**:234–8.
30. Roberson DA, Cui W, Patel D, Tsang W, Sugeng L, Weinert L *et al.* Three-dimensional transesophageal echocardiography of atrial septal defect: a qualitative and quantitative anatomic study. *J Am Soc Echocardiogr* 2011;**24**:600–10.
31. Ojala T, Rosenthal E, Nugent K, Qureshi S, Simpson J. Live 3D echocardiography to guide closure of residual ASD. *JACC Cardiovasc Imaging* 2013;**6**:523–5.
32. Roberson DA, Cui VW. Three-dimensional transesophageal echocardiography of atrial septal defect device closure. *Curr Cardiol Rep* 2014;**16**:453.
33. Saric M, Perk G, Purgess JR, Kronzon I. Imaging atrial septal defects by real-time three-dimensional transesophageal echocardiography: step-by-step approach. *J Am Soc Echocardiogr* 2010;**23**:1128–35.
34. Acar P, Abadir S, Roux D, Taktak A, Dulac Y, Glock Y *et al.* Ebstein's anomaly assessed by real-time 3-D echocardiography. *Ann Thorac Surg* 2006;**82**:731–3.
35. Hadeed K, Hascoet S, Dulac Y, Peyre M, Acar P. Tethering of tricuspid valve resulting from aberrant tendinous cords mimic Ebstein's anomaly, three-dimensional echocardiography approach. *Echocardiography* 2014;**31**:E136–7.
36. Booker OJ, Nanda NC. Echocardiographic assessment of Ebstein's anomaly. *Echocardiography* 2015;**32**(Suppl. 2):S177–88.
37. Badano LP, Agricola E, De Isla LP, Gianfagna P, Zamorano JL. Evaluation of the tricuspid valve morphology and function by transthoracic real-time three-dimensional echocardiography. *Eur J Echocardiogr* 2009;**10**:477–84.
38. Kutty S, Colen T, Thompson RB, Tham E, Li L, Vijarnsorn C *et al.* Tricuspid regurgitation in hypoplastic left heart syndrome: mechanistic insights on tricuspid valve tethering and relationship with outcomes. *Circ Cardiovasc Imaging* 2014;**7**:765–72.
39. van Noord PT, Scohy TV, McGhie J, Bogers AJJC. Three-dimensional transesophageal echocardiography in Ebstein's anomaly. *Interact Cardiovasc Thorac Surg* 2010; **10**:836–7.
40. Kutty S, Smallhorn JF. Evaluation of atrioventricular septal defects by three-dimensional echocardiography: benefits of navigating the third dimension. *J Am Soc Echocardiogr* 2012;**25**:932–44.
41. Takahashi K, Mackie AS, Rebeyka IM, Ross DB, Robertson M, Dyck JD *et al.* Two-dimensional versus transthoracic real-time three-dimensional echocardiography in the evaluation of the mechanisms and sites of atrioventricular valve regurgitation in a congenital heart disease population. *J Am Soc Echocardiogr* 2010;**23**: 726–34.
42. Bharucha T, Anderson RH, Lim ZS, Vettukattil JJ. Multiplanar review of three-dimensional echocardiography gives new insights into the morphology of Ebstein's malformation. *Cardiol Young* 2010;**20**:49–53.
43. Acar P, Abdel-Massih T, Douste-Blazy M-Y, Dulac Y, Bonhoeffer P, Sidi D. Assessment of muscular ventricular septal defect closure by transcatheter or surgical approach: a three-dimensional echocardiographic study. *Eur J Echocardiogr* 2002;**3**: 185–91.
44. Charakida M, Qureshi S, Simpson JM. 3D echocardiography for planning and guidance of interventional closure of VSD. *JACC Cardiovasc Imaging* 2013;**6**:120–3.
45. Chen FL, Hsiung MC, Nanda N, Hsieh KS, Chou MC. Real time three-dimensional echocardiography in assessing ventricular septal defects: an echocardiographic-surgical correlative study. *Echocardiography* 2006;**23**:562–8.
46. Acar P, Abadir S, Aggoun Y. Transcatheter closure of perimembranous ventricular septal defects with Amplatzer occluder assessed by real-time three-dimensional echocardiography. *Eur J Echocardiogr* 2007;**8**:110–5.
47. Sivakumar K, Singhi A, Pavithran S. Enface reconstruction of VSD on RV septal surface using real-time 3D echocardiography. *JACC Cardiovasc Imaging* 2012;**5**: 1176–80.
48. Mercer-Rosa L, Seliem MA, Fedec A, Rome J, Rychik J, Gaynor JW. Illustration of the additional value of real-time 3-dimensional echocardiography to conventional transthoracic and transesophageal 2-dimensional echocardiography in imaging muscular ventricular septal defects: does this have any impact on individual patie. *J Am Soc Echocardiogr* 2006;**19**:1511–9.
49. Maréchaux S, Juthier F, Banfi C, Vincentelli A, Prat A, Ennezat P-V. Illustration of the echocardiographic diagnosis of subaortic membrane stenosis in adults: surgical and live three-dimensional transoesophageal findings. *Eur J Echocardiogr* 2011;**12**:E2.
50. Shirali GS. Three dimensional echocardiography in congenital heart defects. *Ann Pediatr Cardiol* 2008;**1**:8–17.
51. Noel CV, Choy RM, Lester JR, Soriano BD. Accuracy of matrix-array three-dimensional echocardiographic measurements of aortic root dilation and comparison with two-dimensional echocardiography in pediatric patients. *J Am Soc Echocardiogr* 2012;**25**:287–93.
52. Martin R, Hascoët S, Dulac Y, Peyre M, Mejean S, Hadeed K *et al.* Comparison of two- and three-dimensional transthoracic echocardiography for measurement of aortic annulus diameter in children. *Arch Cardiovasc Dis* 2013;**106**:492–500.
53. Hlavacek A, Lucas J, Baker H, Chessa K, Shirali G. Feasibility and utility of three-dimensional color flow echocardiography of the aortic arch: The "echocardiographic angiogram". *Echocardiography* 2006;**23**:860–4.
54. Valente AM, Cook S, Festa P, Ko HH, Krishnamurthy R, Taylor AM *et al.* Multimodality imaging guidelines for patients with repaired tetralogy of fallot: a report from the American Society of Echocardiography: developed in collaboration with the Society for Cardiovascular Magnetic Resonance and the Society for Pediatric Radiology. *J Am Soc Echocardiogr* 2014;**27**:111–41.
55. Anwar AM, Soliman O, van den Bosch AE, McGhie JS, Geleijnse ML, ten Cate FJ *et al.* Assessment of pulmonary valve and right ventricular outflow tract with real-time three-dimensional echocardiography. *Int J Cardiovasc Imaging* 2007;**23**: 167–75.
56. Bharucha T, Sivaprakasam MC, Haw MP, Anderson RH, Vettukattil JJ. The angle of the components of the common atrioventricular valve predicts the outcome of surgical correction in patients with atrioventricular septal defect and common atrioventricular junction. *J Am Soc Echocardiogr* 2008;**21**:1099–104.
57. Faletra FF, Nucifora G, Ho SY. Real-time 3-dimensional transesophageal echocardiography of the atrioventricular septal defect. *Circ Cardiovasc Imaging* 2011;**4**: e7–9.
58. van den Bosch AE, Ten Harkel D-J, McGhie JS, Roos-Hesselink JW, Simoons ML, Bogers AJJC *et al.* Surgical validation of real-time transthoracic 3D echocardiographic assessment of atrioventricular septal defects. *Int J Cardiol* 2006;**112**:213–8.
59. van den Bosch AE, van Dijk VF, McGhie JS, Bogers AJJC, Roos-Hesselink JW, Simoons ML *et al.* Real-time transthoracic three-dimensional echocardiography provides additional information of left-sided AV valve morphology after AVSD repair. *Int J Cardiol* 2006;**106**:360–4.
60. Shirali G, Simpson JM. Pediatric Aspects of Three-Dimensional Echocardiography. In: Lang RM, Shernan SK, Shirali GS, Mor-Avi V, eds.*Comprehensive Atlas of 3D Echocardiography. First.* Philadelphia: Lippincott, Williams and Wilkins; 2012.
61. Abadir S, Léobon B, Acar P. Assessment of tricuspid regurgitation mechanism by three-dimensional echocardiography in an adult patient with congenitally corrected transposition of the great arteries. *Arch Cardiovasc Dis* 2009;**102**:459–60.
62. Kottayil BP, Sunil GS, Kappanayil M, Mohanty SH, Francis E, Vaidyanathan B *et al.* Two-ventricle repair for complex congenital heart defects palliated towards single-ventricle repair. *Interact Cardiovasc Thorac Surg* 2014;**18**:266–71.
63. Del Pasqua A, Sanders SP, De Zorzi A, Toscano A, Iacobelli R, Pierli C *et al.* Impact of three-dimensional echocardiography in complex congenital heart defect cases: the surgical view. *Pediatr Cardiol* 2009;**30**:293–300.
64. Acar P, Saliba Z, Bonhoeffer P, Aggoun Y, Bonnet D, Sidi D *et al.* Influence of atrial septal defect anatomy in patient selection and assessment of closure with the Cardioseal device: a three-dimensional transoesophageal echocardiographic reconstruction. *Eur Heart J* 2000;**21**:573–81.
65. Abdel-Massih T, Dulac Y, Taktak A, Aggoun Y, Massabuau P, Elbaz M *et al.* Assessment of atrial septal defect size with 3D-transesophageal echocardiography: comparison with balloon method. *Echocardiography* 2005;**22**:121–7.
66. Taniguchi M, Akagi T, Kijima Y, Sano S. Clinical advantage of real-time three-dimensional transesophageal echocardiography for transcatheter closure of multiple atrial septal defects. *Int J Cardiovasc Imaging* 2013;**29**:1273–80.
67. Bhaya M, Mutluer FO, Mahan E, Mahan L, Hsiung MC, Yin W-H *et al.* Live/real time three-dimensional transesophageal echocardiography in percutaneous closure of atrial septal defects. *Echocardiography* 2013;**30**:345–53.
68. Cheng TO, Xie M-X, Wang X-F, Wang Y, Lu Q. Real-time 3-dimensional echocardiography in assessing atrial and ventricular septal defects: an echocardiographic-surgical correlative study. *Am Heart J* 2004;**148**:1091–5.
69. van den Bosch AE, Ten Harkel D-J, McGhie JS, Roos-Hesselink JW, Simoons ML, Bogers AJJC *et al.* Feasibility and accuracy of real-time 3-dimensional echocardiographic assessment of ventricular septal defects. *J Am Soc Echocardiogr* 2006;**19**: 7–13.
70. Hsu J-H, Wu J-R, Dai Z-K, Lee M-H. Real-time three-dimensional echocardiography provides novel and useful anatomic insights of perimembranous ventricular septal aneurysm. *Int J Cardiol* 2007;**118**:326–31.
71. Butera G, Biondi-Zoccai G, Sangiorgi G, Abella R, Giamberti A, Bussadori C *et al.* Percutaneous versus surgical closure of secundum atrial septal defects: a

systematic review and meta-analysis of currently available clinical evidence. *EuroIntervention* 2011;**7**:377–85.
72. Du ZD, Hijazi ZM, Kleinman CS, Silverman NH, Larntz K. Comparison between transcatheter and surgical closure of secundum atrial septal defect in children and adults: results of a multicenter nonrandomized trial. *J Am Coll Cardiol* 2002;**39**: 1836–44.
73. Chen FL, Hsiung MC, Hsieh KS, Li YC, Chou MC. Real time three-dimensional transthoracic echocardiography for guiding Amplatzer septal occluder device deployment in patients with atrial septal defect. *Echocardiography* 2006;**23**:763–70.
74. Roman KS, Nii M, Golding F, Benson LN, Smallhorn JF. Images in cardiovascular medicine. Real-time subcostal 3-dimensional echocardiography for guided percutaneous atrial septal defect closure. *Circulation* 2004;**109**:e320–1.
75. Lock JE, Block PC, McKay RG, Baim DS, Keane JF. Transcatheter closure of ventricular septal defects. *Circulation* 1988;**78**:361–8.
76. Knauth AL, Lock JE, Perry SB, McElhinney DB, Gauvreau K, Landzberg MJ *et al.* Transcatheter device closure of congenital and postoperative residual ventricular septal defects. *Circulation* 2004;**110**:501–7.
77. Butera G, Carminati M, Chessa M, Piazza L, Micheletti A, Negura DG *et al.* Transcatheter closure of perimembranous ventricular septal defects: early and long-term results. *J Am Coll Cardiol* 2007;**50**:1189–95.
78. Carminati M, Butera G, Chessa M, De Giovanni J, Fisher G, Gewillig M *et al.* Transcatheter closure of congenital ventricular septal defects: results of the European Registry. *Eur Heart J* 2007;**28**:2361–8.
79. Butera G, Chessa M, Carminati M. Percutaneous closure of ventricular septal defects. State of the art. *J Cardiovasc Med (Hagerstown)* 2007;**8**:39–45.
80. El Said HG, Bratincsak A, Gordon BM, Moore JW. Closure of perimembranous ventricular septal defects with aneurysmal tissue using the Amplazter Duct Occluder I: lessons learned and medium term follow up. *Catheter Cardiovasc Interv* 2012; **80**:895–903.
81. Lucas V. Closure of perimembranous ventricular septal defects with aneurysmal tissue using the Amplazter Duct Occluder I. *Catheter Cardiovasc Interv* 2012;**80**: 904.
82. Giannakoulas G, Thanopoulos V. Three-dimensional transesophageal echocardiography for guiding percutaneous fontan fenestration closure. *Echocardiography* 2014;**31**:E230–1.
83. Raslan S, Nanda NC, Lloyd L, Khairnar P, Reilly SD, Holman WL. Incremental value of live/real time three-dimensional transesophageal echocardiography over the two-dimensional technique in the assessment of sinus of valsalva aneurysm rupture. *Echocardiography* 2011;**28**:918–20.
84. Esper SA, Fink R, Rhodes JF, Harrison JK, Mackensen GB. A coronary artery fistula successfully closed with the precise guidance of three-dimensional echocardiography. *J Cardiothorac Vasc Anesth* 2014;**28**:194–5.
85. Mishra J, Puri HP, Hsiung MC, Misra S, Khairnar P, Laxmi Gollamudi B *et al.* Incremental value of live/real time three-dimensional over two-dimensional transesophageal echocardiography in the evaluation of right coronary artery fistula. *Echocardiography* 2011;**28**:805–8.
86. Singh P, Manda J, Hsiung MC, Mehta A, Kesanolla SK, Nanda NC *et al.* Live/real time three-dimensional transesophageal echocardiographic evaluation of mitral and aortic valve prosthetic paravalvular regurgitation. *Echocardiography* 2009;**26**: 980–7.
87. Cavalcante JL, Rodriguez LL, Kapadia S, Tuzcu EM, Stewart WJ. Role of echocardiography in percutaneous mitral valve interventions. *JACC Cardiovasc Imaging* 2012;**5**:733–46.
88. Alli OO, Hsiung MC, Guvenc T, Neill J, Elguindy M, Ahmed MI *et al.* Incremental value of three-dimensional transesophageal echocardiography over the two-dimensional technique in percutaneous closure of aortic paraprosthetic regurgitation. *Echocardiography* 2014;**31**:1154–8.
89. Cua CL, Kollins K, Roble S, Holzer RJ. Three-dimensional image of a baffle leak in a patient with a mustard operation. *Echocardiography* 2014;**31**:E315–6.
90. Soriano BD, Stout KK, Cailes CD, Jones TK. Transcatether closure of an atrial redirection baffle leak. *Ann Pediatr Cardiol* 2009;**2**:85–6.
91. Faletra FF, Nucifora G, Ho SY. Imaging the atrial septum using real-time three-dimensional transesophageal echocardiography: technical tips, normal anatomy, and its role in transseptal puncture. *J Am Soc Echocardiogr* 2011;**24**:593–9.
92. Döring M, Braunschweig F, Eitel C, Gaspar T, Wetzel U, Nitsche B *et al.* Individually tailored left ventricular lead placement: lessons from multimodality integration between three-dimensional echocardiography and coronary sinus angiogram. *Europace* 2013;**15**:718–27.
93. Fontes-Carvalho R, Sampaio F, Ribeiro J, Gama Ribeiro V. Three-dimensional intracardiac echocardiography: a new promising imaging modality to potentially guide cardiovascular interventions. *Eur Heart J Cardiovasc Imaging* 2013;**14**:1028.
94. Maini B. Real-time three-dimensional intracardiac echocardiography: an early single-center experience. *J Invasive Cardiol* 2015;**27**:E5–12.
95. Silvestry FE, Kadakia MB, Willhide J, Herrmann HC. Initial experience with a novel real-time three-dimensional intracardiac ultrasound system to guide percutaneous cardiac structural interventions: a phase 1 feasibility study of volume intracardiac echocardiography in the assessment of patients with struc. *J Am Soc Echocardiogr* 2014;**27**:978–83.
96. Bellsham-Revell HR, Simpson JM, Miller OI, Bell AJ. Subjective evaluation of right ventricular systolic function in hypoplastic left heart syndrome: how accurate is it? *J Am Soc Echocardiogr* 2013;**26**:52–6.
97. Hoch M, Vasilyev NV, Soriano B, Gauvreau K, Marx GR. Variables influencing the accuracy of right ventricular volume assessment by real-time 3-dimensional echocardiography: an in vitro validation study. *J Am Soc Echocardiogr* 2007;**20**:456–61.
98. Lu X, Nadvoretskiy V, Bu L, Stolpen A, Ayres N, Pignatelli RH *et al.* Accuracy and reproducibility of real-time three-dimensional echocardiography for assessment of right ventricular volumes and ejection fraction in children. *J Am Soc Echocardiogr* 2008;**21**:84–9.
99. Renella P, Marx GR, Zhou J, Gauvreau K, Geva T. Feasibility and reproducibility of three-dimensional echocardiographic assessment of right ventricular size and function in pediatric patients. *J Am Soc Echocardiogr* 2014;**27**:903–10.
100. Maffessanti F, Muraru D, Esposito R, Gripari P, Ermacora D, Santoro C *et al.* Age-, body size-, and sex-specific reference values for right ventricular volumes and ejection fraction by three-dimensional echocardiography: a multicenter echocardiographic study in 507 healthy volunteers. *Circ Cardiovasc Imaging* 2013;**6**:700–10.
101. Tamborini G, Marsan NA, Gripari P, Maffessanti F, Brusoni D, Muratori M *et al.* Reference values for right ventricular volumes and ejection fraction with real-time three-dimensional echocardiography: evaluation in a large series of normal subjects. *J Am Soc Echocardiogr* 2010;**23**:109–15.
102. Leibundgut G, Rohner A, Grize L, Bernheim A, Kessel-Schaefer A, Bremerich J *et al.* Dynamic assessment of right ventricular volumes and function by real-time three-dimensional echocardiography: a comparison study with magnetic resonance imaging in 100 adult patients. *J Am Soc Echocardiogr* 2010;**23**:116–26.
103. Jenkins C, Chan J, Bricknell K, Strudwick M, Marwick TH. Reproducibility of right ventricular volumes and ejection fraction using real-time three-dimensional echocardiography: comparison with cardiac MRI. *Chest* 2007;**131**:1844–51.
104. Dragulescu A, Grosse-Wortmann L, Fackoury C, Mertens L. Echocardiographic assessment of right ventricular volumes: a comparison of different techniques in children after surgical repair of tetralogy of Fallot. *Eur Heart J Cardiovasc Imaging* 2012;**13**:596–604.
105. Grewal J, Majdalany D, Syed I, Pellikka P, Warnes CA. Three-dimensional echocardiographic assessment of right ventricular volume and function in adult patients with congenital heart disease: comparison with magnetic resonance imaging. *J Am Soc Echocardiogr* 2010;**23**:127–33.
106. van der Zwaan HB, Helbing WA, McGhie JS, Geleijnse ML, Luijnenburg SE, Roos-Hesselink JW *et al.* Clinical value of real-time three-dimensional echocardiography for right ventricular quantification in congenital heart disease: validation with cardiac magnetic resonance imaging. *J Am Soc Echocardiogr* 2010;**23**:134–40.
107. van der Zwaan HB, Geleijnse ML, Soliman OII, McGhie JS, Wiegers-Groeneweg EJA, Helbing WA *et al.* Test-retest variability of volumetric right ventricular measurements using real-time three-dimensional echocardiography. *J Am Soc Echocardiogr* 2011;**24**:671–9.
108. Iriart X, Montaudon M, Lafitte S, Chabaneix J, Réant P, Balbach T *et al.* Right ventricle three-dimensional echography in corrected tetralogy of Fallot: accuracy and variability. *Eur J Echocardiogr* 2009;**10**:784–92.
109. Grapsa J, O'Regan DP, Pavlopoulos H, Durighel G, Dawson D, Nihoyannopoulos P. Right ventricular remodelling in pulmonary arterial hypertension with three-dimensional echocardiography: comparison with cardiac magnetic resonance imaging. *Eur J Echocardiogr* 2010;**11**:64–73.
110. Dragulescu A, Grosse-Wortmann L, Fackoury C, Riffle S, Waiss M, Jaeggi E *et al.* Echocardiographic assessment of right ventricular volumes after surgical repair of tetralogy of Fallot: clinical validation of a new echocardiographic method. *J Am Soc Echocardiogr* 2011;**24**:1191–8.
111. Kutty S, Li L, Polak A, Gribben P, Danford DA. Echocardiographic knowledge-based reconstruction for quantification of the systemic right ventricle in young adults with repaired D-transposition of great arteries. *Am J Cardiol* 2012;**109**: 881–8.
112. Zhang QB, Sun JP, Gao RF, Lee AP-W, Feng YL, Liu XR *et al.* Feasibility of single-beat full-volume capture real-time three-dimensional echocardiography for quantification of right ventricular volume: validation by cardiac magnetic resonance imaging. *Int J Cardiol* 2013;**168**:3991–5.
113. Friedberg MK, Su X, Tworetzky W, Soriano BD, Powell AJ, Marx GR. Validation of 3D echocardiographic assessment of left ventricular volumes, mass, and ejection fraction in neonates and infants with congenital heart disease: a comparison study with cardiac MRI. *Circ Cardiovasc Imaging* 2010;**3**:735–42.
114. Selly J-B, Iriart X, Roubertie F, Mauriat P, Marek J, Guilhon E *et al.* Multivariable assessment of the right ventricle by echocardiography in patients with repaired tetralogy of Fallot undergoing pulmonary valve replacement: a comparative study with magnetic resonance imaging. *Arch Cardiovasc Dis* 2015;**108**:5–15.

115. Kutty S, Graney BA, Khoo NS, Li L, Polak A, Gribben P *et al.* Serial assessment of right ventricular volume and function in surgically palliated hypoplastic left heart syndrome using real-time transthoracic three-dimensional echocardiography. *J Am Soc Echocardiogr* 2012;**25**:682–9.
116. Bell A, Rawlins D, Bellsham-Revell H, Miller O, Razavi R, Simpson J. Assessment of right ventricular volumes in hypoplastic left heart syndrome by real-time three-dimensional echocardiography: comparison with cardiac magnetic resonance imaging. *Eur Heart J Cardiovasc Imaging* 2014;**15**:257–66.
117. Hubka M, Bolson EL, McDonald JA, Martin RW, Munt B, Sheehan FH. Three-dimensional echocardiographic measurement of left and right ventricular mass and volume: in vitro validation. *Int J Cardiovasc Imaging* 2002;**18**:111–8.
118. Sheehan FH, Kilner PJ, Sahn DJ, Vick GW, Stout KK, Ge S *et al.* Accuracy of knowledge-based reconstruction for measurement of right ventricular volume and function in patients with tetralogy of Fallot. *Am J Cardiol* 2010;**105**:993–9.
119. Moroseos T, Mitsumori L, Kerwin WS, Sahn DJ, Helbing WA, Kilner PJ *et al.* Comparison of Simpson's method and three-dimensional reconstruction for measurement of right ventricular volume in patients with complete or corrected transposition of the great arteries. *Am J Cardiol* 2010;**105**:1603–9.
120. Bhave NM, Patel AR, Weinert L, Yamat M, Freed BH, Mor-Avi V *et al.* Three-dimensional modeling of the right ventricle from two-dimensional transthoracic echocardiographic images: utility of knowledge-based reconstruction in pulmonary arterial hypertension. *J Am Soc Echocardiogr* 2013;**26**:860–7.
121. Leary PJ, Kurtz CE, Hough CL, Waiss M-P, Ralph DD, Sheehan FH. Three-dimensional analysis of right ventricular shape and function in pulmonary hypertension. *Pulm Circ* 2012;**2**:34–40.
122. van den Bosch AE, Robbers-Visser D, Krenning BJ, Voormolen MM, McGhie JS, Helbing WA *et al.* Real-time transthoracic three-dimensional echocardiographic assessment of left ventricular volume and ejection fraction in congenital heart disease. *J Am Soc Echocardiogr* 2006;**19**:1–6.
123. Shimada YJ, Shiota T. A meta-analysis and investigation for the source of bias of left ventricular volumes and function by three-dimensional echocardiography in comparison with magnetic resonance imaging. *Am J Cardiol* 2011;**107**:126–38.
124. Altmann K, Shen Z, Boxt LM, King DL, Gersony WM, Allan LD *et al.* Comparison of three-dimensional echocardiographic assessment of volume, mass, and function in children with functionally single left ventricles with two-dimensional echocardiography and magnetic resonance imaging. *Am J Cardiol* 1997;**80**:1060–5.
125. Bu L, Munns S, Zhang H, Disterhoft M, Dixon M, Stolpen A *et al.* Rapid full volume data acquisition by real-time 3-dimensional echocardiography for assessment of left ventricular indexes in children: a validation study compared with magnetic resonance imaging. *J Am Soc Echocardiogr* 2005;**18**:299–305.
126. Riehle TJ, Mahle WT, Parks WJ, Sallee D, Fyfe DA. Real-time three-dimensional echocardiographic acquisition and quantification of left ventricular indices in children and young adults with congenital heart disease: comparison with magnetic resonance imaging. *J Am Soc Echocardiogr* 2008;**21**:78–83.
127. Lu X, Xie M, Tomberlin D, Klas B, Nadvoretskiy V, Ayres N *et al.* How accurately, reproducibly, and efficiently can we measure left ventricular indices using M-mode, 2-dimensional, and 3-dimensional echocardiography in children? *Am Heart J* 2008;**155**:946–53.
128. Laser KT, Bunge M, Hauffe P, Argueta JRP, Kelter-Klöpping A, Barth P *et al.* Left ventricular volumetry in healthy children and adolescents: comparison of two different real-time three-dimensional matrix transducers with cardiovascular magnetic resonance. *Eur J Echocardiogr* 2010;**11**:138–48.
129. Poutanen T, Ikonen A, Jokinen E, Vainio P, Tikanoja T. Transthoracic three-dimensional echocardiography is as good as magnetic resonance imaging in measuring dynamic changes in left ventricular volume during the heart cycle in children. *Eur J Echocardiogr* 2001;**2**:31–9.
130. Ylänen K, Eerola A, Vettenranta K, Poutanen T. Three-dimensional echocardiography and cardiac magnetic resonance imaging in the screening of long-term survivors of childhood cancer after cardiotoxic therapy. *Am J Cardiol* 2014;**113**:1886–92.
131. Balluz R, Liu L, Zhou X, Ge S. Real time three-dimensional echocardiography for quantification of ventricular volumes, mass, and function in children with congenital and acquired heart diseases. *Echocardiography* 2013;**30**:472–82.
132. Poutanen T, Jokinen E. Left ventricular mass in 169 healthy children and young adults assessed by three-dimensional echocardiography. *Pediatr Cardiol* 2007;**28**:201–7.
133. Foster BJ, Mackie AS, Mitsnefes M, Ali H, Mamber S, Colan SD. A novel method of expressing left ventricular mass relative to body size in children. *Circulation* 2008;**117**:2769–75.
134. Khoury PR, Mitsnefes M, Daniels SR, Kimball TR. Age-specific reference intervals for indexed left ventricular mass in children. *J Am Soc Echocardiogr* 2009;**22**:709–14.
135. van den Bosch AE, Robbers-Visser D, Krenning BJ, McGhie JS, Helbing WA, Meijboom FJ *et al.* Comparison of real-time three-dimensional echocardiography to magnetic resonance imaging for assessment of left ventricular mass. *Am J Cardiol* 2006;**97**:113–7.
136. Kapetanakis S, Kearney MT, Siva A, Gall N, Cooklin M, Monaghan MJ. Real-time three-dimensional echocardiography: a novel technique to quantify global left ventricular mechanical dyssynchrony. *Circulation* 2005;**112**:992–1000.
137. Cui W, Gambetta K, Zimmerman F, Freter A, Sugeng L, Lang R *et al.* Real-time three-dimensional echocardiographic assessment of left ventricular systolic dyssynchrony in healthy children. *J Am Soc Echocardiogr* 2010;**23**:1153–9.
138. Ten Harkel ADJ, Van Osch-Gevers M, Helbing WA. Real-time transthoracic three dimensional echocardiography: normal reference data for left ventricular dyssynchrony in adolescents. *J Am Soc Echocardiogr* 2009;**22**:933–8.
139. Ojala T, Mathur S, Vatanen A, Sinha MD, Jahnukainen K, Simpson J. Repeatability and agreement of real time three-dimensional echocardiography measurements of left ventricular mass and synchrony in young patients. *Echocardiography* 2015;**32**:522–7.
140. Yu Y, Sun K, Xue H, Chen S, Yang J. Usefulness of real-time 3-dimensional echocardiography to identify and quantify left ventricular dyssynchrony in patients with Kawasaki disease. *J Ultrasound Med* 2013;**32**:1013–21.
141. Baker GH, Hlavacek AM, Chessa KS, Fleming DM, Shirali GS. Left ventricular dysfunction is associated with intraventricular dyssynchrony by 3-dimensional echocardiography in children. *J Am Soc Echocardiogr* 2008;**21**:230–3.
142. Ho P-K, Lai CTM, Wong SJ, Cheung Y-F. Three-dimensional mechanical dyssynchrony and myocardial deformation of the left ventricle in patients with tricuspid atresia after Fontan procedure. *J Am Soc Echocardiogr* 2012;**25**:393–400.
143. Raedle-Hurst TM, Mueller M, Rentzsch A, Schaefers H-J, Herrmann E, Abdul-Khaliq H. Assessment of left ventricular dyssynchrony and function using real-time 3-dimensional echocardiography in patients with congenital right heart disease. *Am Heart J* 2009;**157**:791–8.
144. Sonne C, Sugeng L, Takeuchi M, Weinert L, Childers R, Watanabe N *et al.* Real-time 3-dimensional echocardiographic assessment of left ventricular dyssynchrony: pitfalls in patients with dilated cardiomyopathy. *JACC Cardiovasc Imaging* 2009;**2**:802–12.
145. Wu VC-C, Takeuchi M, Otani K, Haruki N, Yoshitani H, Tamura M *et al.* Effect of through-plane and twisting motion on left ventricular strain calculation: direct comparison between two-dimensional and three-dimensional speckle-tracking echocardiography. *J Am Soc Echocardiogr* 2013;**26**:1274–81.e4.
146. Kaku K, Takeuchi M, Tsang W, Takigiku K, Yasukochi S, Patel AR *et al.* Age-related normal range of left ventricular strain and torsion using three-dimensional speckle-tracking echocardiography. *J Am Soc Echocardiogr* 2014;**27**:55–64.
147. Zhang L, Gao J, Xie M, Yin P, Liu W, Li Y *et al.* Left ventricular three-dimensional global systolic strain by real-time three-dimensional speckle-tracking in children: feasibility, reproducibility, maturational changes, and normal ranges. *J Am Soc Echocardiogr* 2013;**26**:853–9.
148. Yao C, Simpson JM, Schaeffter T, Penney GP. Multi-view 3D echocardiography compounding based on feature consistency. *Phys Med Biol* 2011;**56**:6109–28.
149. Said SM, Dearani JA, Burkhart HM, Connolly HM, Eidem B, Stensrud PE *et al.* Management of tricuspid regurgitation in congenital heart disease: is survival better with valve repair? *J Thorac Cardiovasc Surg* 2014;**147**:412–7.
150. Yamagishi S, Masuoka A, Uno Y, Katogi T, Suzuki T. Influence of bidirectional cavopulmonary anastomosis and concomitant valve repair on atrioventricular valve annulus and function. *Ann Thorac Surg* 2014;**98**:641–7.
151. Swanson JC, Krishnamurthy G, Kvitting J-PE, Miller DC, Ingels NB. Electromechanical coupling between the atria and mitral valve. *Am J Physiol Heart Circ Physiol* 2011;**300**:H1267–73.
152. Salgo IS, Gorman JH, Gorman RC, Jackson BM, Bowen FW, Plappert T *et al.* Effect of annular shape on leaflet curvature in reducing mitral leaflet stress. *Circulation* 2002;**106**:711–7.
153. Nii M, Roman KS, Macgowan CK, Smallhorn JF. Insight into normal mitral and tricuspid annular dynamics in pediatrics: a real-time three-dimensional echocardiographic study. *J Am Soc Echocardiogr* 2005;**18**:805–14.
154. Ando M, Takahashi Y. Variations of atrioventricular septal defects predisposing to regurgitation and stenosis. *Ann Thorac Surg* 2010;**90**:614–21.
155. Kanani M, Elliott M, Cook A, Juraszek A, Devine W, Anderson RH. Late incompetence of the left atrioventricular valve after repair of atrioventricular septal defects: the morphologic perspective. *J Thorac Cardiovasc Surg* 2006;**132**:640–6.
156. Krishnamurthy G, Itoh A, Swanson JC, Miller DC, Ingels NB. Transient stiffening of mitral valve leaflets in the beating heart. *Am J Physiol Heart Circ Physiol* 2010;**298**:H2221–5.
157. Swanson JC, Krishnamurthy G, Itoh A, Kvitting J-PE, Bothe W, Craig Miller D *et al.* Multiple mitral leaflet contractile systems in the beating heart. *J Biomech* 2011;**44**:1328–33.
158. Takahashi K, Inage A, Rebeyka IM, Ross DB, Thompson RB, Mackie AS *et al.* Real-time 3-dimensional echocardiography provides new insight into mechanisms of tricuspid valve regurgitation in patients with hypoplastic left heart syndrome. *Circulation* 2009;**120**:1091–8.

159. Takahashi K, Mackie AS, Thompson R, Al-Naami G, Inage A, Rebeyka IM *et al.* Quantitative real-time three-dimensional echocardiography provides new insight into the mechanisms of mitral valve regurgitation post-repair of atrioventricular septal defect. *J Am Soc Echocardiogr* 2012;**25**:1231–44.
160. Ypenburg C, Lancellotti P, Tops LF, Bleeker GB, Holman ER, Piérard LA *et al.* Acute effects of initiation and withdrawal of cardiac resynchronization therapy on papillary muscle dyssynchrony and mitral regurgitation. *J Am Coll Cardiol* 2007;**50**:2071–7.
161. Bharucha T, Khan R, Mertens L, Friedberg MK. Right ventricular mechanical dyssynchrony and asymmetric contraction in hypoplastic heart syndrome are associated with tricuspid regurgitation. *J Am Soc Echocardiogr* 2013;**26**:1214–20.
162. Takahashi K, Guerra V, Roman KS, Nii M, Redington A, Smallhorn JF. Three-dimensional echocardiography improves the understanding of the mechanisms and site of left atrioventricular valve regurgitation in atrioventricular septal defect. *J Am Soc Echocardiogr* 2006;**19**:1502–10.
163. Nii M, Guerra V, Roman KS, Macgowan CK, Smallhorn JF. Three-dimensional tricuspid annular function provides insight into the mechanisms of tricuspid valve regurgitation in classic hypoplastic left heart syndrome. *J Am Soc Echocardiogr* 2006; **19**:391–402.
164. Colen TM, Khoo NS, Ross DB, Smallhorn JF. Partial zone of apposition closure in atrioventricular septal defect: are papillary muscles the clue. *Ann Thorac Surg* 2013; **96**:637–43.
165. Kusunose K, Cremer PC, Tsutsui RS, Grimm RA, Thomas JD, Griffin BP *et al.* Regurgitant volume informs rate of progressive cardiac dysfunction in asymptomatic patients with chronic aortic or mitral regurgitation. *JACC Cardiovasc Imaging* 2014; **8**:14–23.
166. Thomas N, Unsworth B, Ferenczi EA, Davies JE, Mayet J, Francis DP. Intraobserver variability in grading severity of repeated identical cases of mitral regurgitation. *Am Heart J* 2008;**156**:1089–94.
167. Zoghbi WA, Enriquez-Sarano M, Foster E, Grayburn PA, Kraft CD, Levine RA *et al.* Recommendations for evaluation of the severity of native valvular regurgitation with two-dimensional and Doppler echocardiography. *J Am Soc Echocardiogr* 2003;**16**:777–802.
168. Lancellotti P, Moura L, Pierard LA, Agricola E, Popescu BA, Tribouilloy C *et al.* European Association of Echocardiography recommendations for the assessment of valvular regurgitation. Part 2: mitral and tricuspid regurgitation (native valve disease). *Eur J Echocardiogr* 2010;**11**:307–32.
169. Choi J, Heo R, Hong G-R, Chang H-J, Sung JM, Shin SH *et al.* Differential effect of 3-dimensional color Doppler echocardiography for the quantification of mitral regurgitation according to the severity and characteristics. *Circ Cardiovasc Imaging* 2014;**7**:535–44.
170. Prakash A, Lacro RV, Sleeper LA, Minich LL, Colan SD, McCrindle B *et al.* Challenges in echocardiographic assessment of mitral regurgitation in children after repair of atrioventricular septal defect. *Pediatr Cardiol* 2012;**33**:205–14.
171. Biner S, Rafique A, Rafii F, Tolstrup K, Noorani O, Shiota T *et al.* Reproducibility of proximal isovelocity surface area, vena contracta, and regurgitant jet area for assessment of mitral regurgitation severity. *JACC Cardiovasc Imaging* 2010;**3**:235–43.
172. Thavendiranathan P, Liu S, Datta S, Walls M, Nitinunu A, Van Houten T *et al.* Automated quantification of mitral inflow and aortic outflow stroke volumes by three-dimensional real-time volume color-flow Doppler transthoracic echocardiography: comparison with pulsed-wave Doppler and cardiac magnetic resonance imaging. *J Am Soc Echocardiogr* 2012;**25**:56–65.
173. Ge S, Bu L, Zhang H, Schelbert E, Disterhoft M, Li X *et al.* A real-time 3-dimensional digital Doppler method for measurement of flow rate and volume through mitral valve in children: a validation study compared with magnetic resonance imaging. *J Am Soc Echocardiogr* 2005;**18**:1–7.
174. Lu X, Nadvoretskiy V, Klas B, Bu L, Stolpen A, Ayres NA *et al.* Measurement of volumetric flow by real-time 3-dimensional Doppler echocardiography in children. *J Am Soc Echocardiogr* 2007;**20**:915–20.
175. Maragiannis D, Little SH. 3D vena contracta area to quantify severity of mitral regurgitation: a practical new tool? *Hellenic J Cardiol* 2013;**54**:448–54.
176. Lancellotti P, Tribouilloy C, Hagendorff A, Moura L, Popescu BA, Agricola E *et al.* European Association of Echocardiography recommendations for the assessment of valvular regurgitation. Part 1: aortic and pulmonary regurgitation (native valve disease). *Eur J Echocardiogr* 2010;**11**:223–44.
177. Vahanian A, Alfieri O, Andreotti F, Antunes MJ, Barón-Esquivias G, Baumgartner H *et al.* Guidelines on the management of valvular heart disease (version 2012). *Eur Heart J* 2012;**33**:2451–96.
178. Cognet T, Séguéla P-E, Thomson E, Bouisset F, Lairez O, Hascoët S *et al.* Assessment of valvular surfaces in children with a congenital bicuspid aortic valve: preliminary three-dimensional echocardiographic study. *Arch Cardiovasc Dis* 2013;**106**:295–302.
179. Poutanen T, Tikanoja T, Sairanen H, Jokinen E. Normal mitral and aortic valve areas assessed by three- and two-dimensional echocardiography in 168 children and young adults. *Pediatr Cardiol* 2006;**27**:217–25.
180. Perez de Isla L, Zamorano J, Fernandez-Golfin C, Ciocarelli S, Corros C, Sanchez T *et al.* 3D color-Doppler echocardiography and chronic aortic regurgitation: a novel approach for severity assessment. *Int J Cardiol* 2013;**166**:640–5.
181. Ewe SH, Delgado V, van der Geest R, Westenberg JJM, Haeck MLA, Witkowski TG *et al.* Accuracy of three-dimensional versus two-dimensional echocardiography for quantification of aortic regurgitation and validation by three-dimensional three-directional velocity-encoded magnetic resonance imaging. *Am J Cardiol* 2013;**112**:560–6.
182. Calleja A, Thavendiranathan P, Ionasec RI, Houle H, Liu S, Voigt I *et al.* Automated quantitative 3-dimensional modeling of the aortic valve and root by 3-dimensional transesophageal echocardiography in normals, aortic regurgitation, and aortic stenosis: comparison to computed tomography in normals and clinical implications. *Circ Cardiovasc Imaging* 2013;**6**:99–108.
183. Festa P, Ait-Ali L, Minichilli F, Kristo I, Deiana M, Picano E. A new simple method to estimate pulmonary regurgitation by echocardiography in operated fallot: comparison with magnetic resonance imaging and performance test evaluation. *J Am Soc Echocardiogr* 2010;**23**:496–503.
184. Pothineni KR, Wells BJ, Hsiung MC, Nanda NC, Yelamanchili P, Suwanjutah T *et al.* Live/real time three-dimensional transthoracic echocardiographic assessment of pulmonary regurgitation. *Echocardiography* 2008;**25**:911–7.
185. Sanders SP, Colan SD, Cordes TM, Donofrio MT, Ensing GJ, Geva T *et al.* ACCF/AHA/AAP recommendations for training in pediatric cardiology. Task force 2: pediatric training guidelines for noninvasive cardiac imaging endorsed by the American Society of Echocardiography and the Society of Pediatric Echocardiography. *J Am Coll Cardiol* 2005;**46**:1384–8.
186. Mertens L, Seri I, Marek J, Arlettaz R, Barker P, McNamara P *et al.* Targeted neonatal echocardiography in the neonatal intensive care unit: practice guidelines and recommendations for training:. *Eur J Echocardiogr* 2011;**12**:715–36.
187. Mertens L, Helbing W, Sieverding L, Daniels O. Guidelines from the Association for European Paediatric Cardiology: standards for training in paediatric echocardiography. *Cardiol Young* 2005;**15**:441–2.
188. Mertens L, Miller O, Fox K, Simpson J. Certification in echocardiography of congenital heart disease: experience of the first 6 years of a European process. *Eur Heart J Cardiovasc Imaging* 2013;**14**:142–8.
189. Pellikka PA, Douglas PS, Miller JG, Abraham TP, Baumann R, Buxton DB *et al.* American Society of Echocardiography Cardiovascular Technology and Research Summit: a roadmap for 2020. *J Am Soc Echocardiogr* 2013;**26**:325–38.
190. Bose RR, Matyal R, Warraich HJ, Summers J, Subramaniam B, Mitchell J *et al.* Utility of a transesophageal echocardiographic simulator as a teaching tool. *J Cardiothorac Vasc Anesth* 2011;**25**:212–5.
191. Jelacic S, Bowdle A, Togashi K, VonHomeyer P. The use of TEE simulation in teaching basic echocardiography skills to senior anesthesiology residents. *J Cardiothorac Vasc Anesth* 2013;**27**:670–5.
192. Jenkins C, Monaghan M, Shirali G, Guraraja R, Marwick TH. An intensive interactive course for 3D echocardiography: is "crop till you drop" an effective learning strategy? *Eur J Echocardiogr* 2008;**9**:373–80.
193. Srivastava S, Printz BF, Geva T, Shirali GS, Weinberg PM, Wong PC *et al.* Task force 2: pediatric cardiology fellowship training in noninvasive cardiac imaging. *J Am Coll Cardiol* 2015;**66**:687–98.
194. Perrin DP, Vasilyev NV, Marx GR, del Nido PJ. Temporal enhancement of 3D echocardiography by frame reordering. *JACC Cardiovasc Imaging* 2012;**5**:300–4.
195. de Vecchi A, Gomez A, Pushparajah K, Schaeffter T, Nordsletten DA, Simpson JM *et al.* Towards a fast and efficient approach for modelling the patient-specific ventricular haemodynamics. *Prog Biophys Mol Biol* 2014;**116**:3–10.
196. Gomez A, De Vecchi A, Jantsch M, Shi W, Pushparajah K, Simpson J *et al.* 4D blood flow reconstruction over the entire ventricle from wall motion and blood velocity derived from ultrasound data. *IEEE Trans Med Imaging* 2015;**34**:2298–308.
197. Olivieri LJ, Krieger A, Loke Y-H, Nath DS, Kim PCW, Sable CA. Three-dimensional printing of intracardiac defects from three-dimensional echocardiographic images: feasibility and relative accuracy. *J Am Soc Echocardiogr* 2015;**28**: 392–7.
198. Samuel BP, Pinto C, Pietila T, Vettukattil JJ. Ultrasound-derived three-dimensional printing in congenital heart disease. *J Digit Imaging* 2015;**28**:459–61.